DOKUZ EYLÜL UNIVERSITY
GRADUATE SCHOOL OF NATURAL AND APPLIED SCIENCES

FABRICATION AND CHARACTERIZATION OF PEDOT: PSS-BASED COMPOSITE FILMS

by
Şeyma ÖZKAN

June, 2024
İZMİR

FABRICATION AND CHARACTERIZATION OF PEDOT: PSS-BASED COMPOSITE FILMS

A Thesis Submitted to the
Graduate School of Natural and Applied Sciences of Dokuz Eylül University
In Partial Fulfillment of the Requirements for Master of Science in
Department of Chemistry, Chemistry Master's Program

by
Şeyma ÖZKAN

June, 2024
İZMİR

M.Sc THESIS EXAMINATION RESULT FORM

We have read the thesis entitled **"FABRICATION AND CHARACTERIZATION OF PEDOT: PSS-BASED COMPOSITE FILMS"** completed by **Şeyma ÖZKAN** under supervision of **PROF.DR. Yoldaş SEKİ** and **Assist. Prof. Dr. Gökhan GÜRLEK** we certify that in our opinion it is fully adequate, in scope and in quality, as a thesis for the degree of Master of Science.

Prof. Dr. Yoldaş SEKİ	Assist. Prof. Dr. Gökhan GÜRLEK
Supervisor	Co-Supervisor
Assoc. Prof. Dr. Aylin ALTINIŞIK TAĞAÇ	Assist. Prof. Dr. Mert ŞENER
Jury Member	Jury Member

Assoc. Prof. Dr. Mehmet Akif EZAN

Jury Member

Prof. Dr. Okan FISTIKOĞLU

Director

Graduate School of Natural and Applied Sciences

ACKNOWLEDGMENT

I extend my heartfelt thanks to my thesis advisor, Prof. Dr. Yoldaş SEKİ, who has been by my side at every stage of my thesis and has never withheld his support. Without his knowledge and guidance, I could not have completed this journey.

I am indebted to Assist. Prof. Dr. Gökhan GÜRLEK, my co-supervisor, who has guided me in every aspect of my work and with whom I am pleased to collaborate. Assist. Prof. Dr. GÜRLEK is not only an academic but also a valuable mentor to me.

I would like to express my gratitude to Assist. Prof. Dr. Barış Oğuz GÜRSES, who generously assisted me during my studies at the MrML laboratory of Ege University Mechanical Engineering Department. Additionally, I extend my thanks to Assist. Prof. Dr. Aysun BALTACI, for the value she placed on me and for always being constructive in her comments, words, and attitudes.

I express my gratitude to Hicran BEŞİKCİ, whose presence I felt despite the distance, I would like to thank Assist. Prof. Dr. Mert ŞENER, who helped me in my work as much as my thesis advisors and made me feel his support under all circumstances.

I am grateful to Oktay ALKAN, who patiently explained to me how to rectify my forgotten and erroneous course selections and never withheld his assistance whenever I encountered school-related issues.

Lastly, I cannot thank enough my husband and closest friend, Dr. Bekir ÖZKAN, who served as an inspiration for me to pursue my master's degree, offered different perspectives in my academic endeavors, and was the first person I turned to whenever I faced any problems in my life.

The thesis was supported by TÜBİTAK project number 121M532.

Şeyma ÖZKAN

FABRICATION AND CHARACTERIZATION OF PEDOT: PSS-BASED COMPOSITE FILMS

ABSTRACT

Energy usage, sustainability, and efficient utilization of energy resources are of great importance today. Consequently, efforts to recover energy and obtain energy from waste heat are increasing. Thermoelectricity emerges as an option for efficient energy utilization. Thermoelectric systems operate on the principle of utilizing temperature differences to generate electricity or, conversely, creating temperature differentials by applying potential differences. In recent years, the use of polymer-based thermoelectric materials has become a research focus. Polymers such as polythiophene-based PEDOT:PSS(Poly(3,4-ethylenedioxythiophene)-poly (styrene sulfonate)) stand out due to their low cost, flexibility, and processability. However, polymers alone may not provide sufficient power generation. Hence, various dopants are used to enhance their performance. Dopants like DMSO(dimethyl sulfoksit), EG(ethylene glycol), PEG(polyethylene glycol) can improve the electrical conductivity of PEDOT:PSS, thus enhancing thermoelectric efficiency. The concentration of PEDOT:PSS in polymer solutions significantly influences the material's electrical properties, with higher concentrations leading to increased electrical conductivity. Additionally, the addition of semiconducting materials (such as silver selenide) allows for control of the electron and hole distribution, which can affect thermoelectric performance. The aim of these studies is to understand the effects of different materials added to polymer solutions on their electrical conductivity and thermoelectric properties, contributing to the development of more efficient thermoelectric modules. With future module studies, the best energy harvest will be achieved from the systems used with high-performance thermoelectric modules.

Keywords: PEDOT: PSS, Thermoelectricity, Electrical Conductivity, Seebeck coefficient, Ag_2Se

PEDOT: PSS TABANLI KOMPOZİT FILMLERIN ÜRETİMİ VE KARAKTERİZASYONU

ÖZ

Günümüzde enerji kullanımı, sürdürülebilirlik ve enerji kaynaklarının verimli kullanımı açısından büyük bir öneme sahiptir. Bu durumda, enerjinin geri kazanımı ve atık ısıdan enerji elde etme çabaları giderek artmaktadır. Termoelektrik, enerjinin verimli kullanımı konusunda bir seçenek olarak öne çıkmaktadır. Termoelektrik sistemler, sıcaklık farkı kullanarak elektrik üretme veya tam tersi olarak potansiyel fark oluşturarak sıcaklık elde etme prensibine dayanır. Son yıllarda, polimer tabanlı termoelektrik malzemelerin kullanımı araştırma alanı haline gelmiştir. Politiyofen kökenli PEDOT:PSS(Poly(3,4-ethylenedioxythiophene)-poly (styrene sulfonate)) gibi polimerler, düşük maliyetleri, esneklikleri ve işlenebilirlikleri nedeniyle dikkat çekmektedir. Ancak polimerlerden yeteri kadar güç eldesi sağlanamamaktadır. Bu durumda, bu polimerlerin performansını artırmak için çeşitli dopantlar kullanılmaktadır. Örneğin, DMSO(dimethyl sulfoxide), EG(etilen glikol), PEG(poli etilen glikol) gibi katkı malzemeleri PEDOT:PSS malzemesinin elektriksel iletkenliğini ve dolayısıyla termoelektrik verimliliğini artırabilir. Polimer çözeltilerindeki PEDOT:PSS konsantrasyonu, malzemenin elektriksel özelliklerini büyük ölçüde etkiler. Bu konsantrasyon arttıkça, malzemenin elektriksel iletkenliği de artar. Ayrıca, yarıiletken malzemelerin (örneğin, gümüş selenür gibi) eklenmesiyle malzemenin elektron ve boşluk dağılımı kontrol edilebilir, bu da termoelektrik performansı üzerinde etkili olabilir. Bu çalışmaların amacı, polimer çözeltilerine eklenen farklı malzemelerin elektriksel iletkenlik ve termoelektrik özellikleri üzerindeki etkilerini anlamak ve daha verimli termoelektrik modüllerin geliştirilmesine katkıda bulunmaktır. Bu şekilde, gelecekte enerji hasadı ve dönüşümünde daha etkin ve verimli sistemlerin kullanılması hedeflenmektedir.

Anahtar kelimeler: PEDOT: PSS, Termoelektrik, Elektriksel İletkenlik, Seebeck Katsayısı, Ag_2Se

CONTENTS

Page

LIST OF FIGURES

Page

LIST OF TABLES

Page

LIST OF SYMBOLS

℃	: Centigrade
%	: Percentage
mm	: Millimeter
º	: Degree
wt.	: Weight
PF	: Power Factor
ΔT	: Different Temperature
μV	: Microvolt
S	: Siemens
K	: Kelvin

ABBREVIATIONS

EDOT	: 3,4-Ethylenedioxythiophene
PEDOT: PSS	: Poly(3,4-ethylenedioxythiophene)-poly (styrene sulfonate)
GR	: Graphene
CNTMW	: Multi Walled Carbon Nanotube
DMSO	: dimethyl Sulfoxide
EG	: Ethylene Glycol
PEG	: Polyethylene Glycol
PVC	: Polyvinyl chloride
PET	: Polyethylene Terephthalate
PDMS	: Polydimethylsiloxane
PP	: Poly Propylene
PC	: Poly carbonate
Ag_2Se	: Silver selenide
$CuCl_2$	: Cupper Chloride
SEM	: Scanning electron microscopy
EDX	: Energy-dispersive X-ray spectroscopy
IEA	: International Energy Agency

CHAPTER ONE
INTRODUCTION

In recent years, there has been significant emphasis on research and efforts towards clean energy production due to increasing energy demand, environmental impacts, and limited resources. The adverse environmental effects of fossil fuel usage, along with factors such as global warming and air pollution, have underscored the importance of renewable energy sources (Manjunath & Kaushik, 2014). Consequently, interest and investments in renewable sources like solar energy, wind energy, and hydroelectric power have increased. Additionally, enhancing energy efficiency has become crucial, as it can reduce energy consumption and minimize environmental impacts. Figure 1.1 illustrates the variation in the use of energy sources for electricity generation over the years.

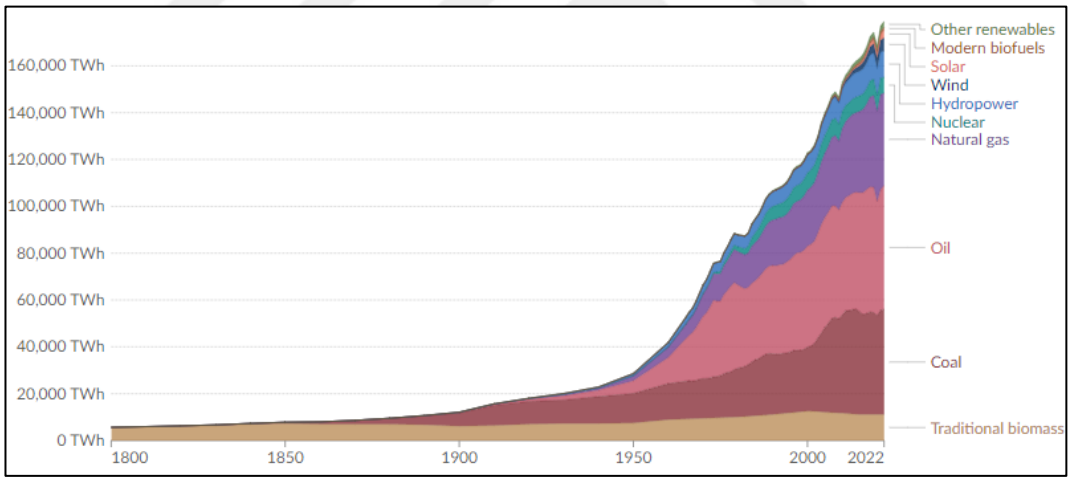

Figure 1.1 The use of energy sources for electricity generation over the years

Since the 1950s, the bulk of energy production has been derived from carbon-based sources like coal, petroleum, and natural gas. While renewable energy sources have shown an increase in recent years, it has not been substantial enough to surpass fossil fuels. Increasing the utilization of alternative energy sources is one approach to reducing fossil fuel consumption. However, one of the foremost challenges the world

confronts is energy efficiency. Figure 1.2 illustrates energy efficiency trends over the years (Ritchie & Rosado, 2020).

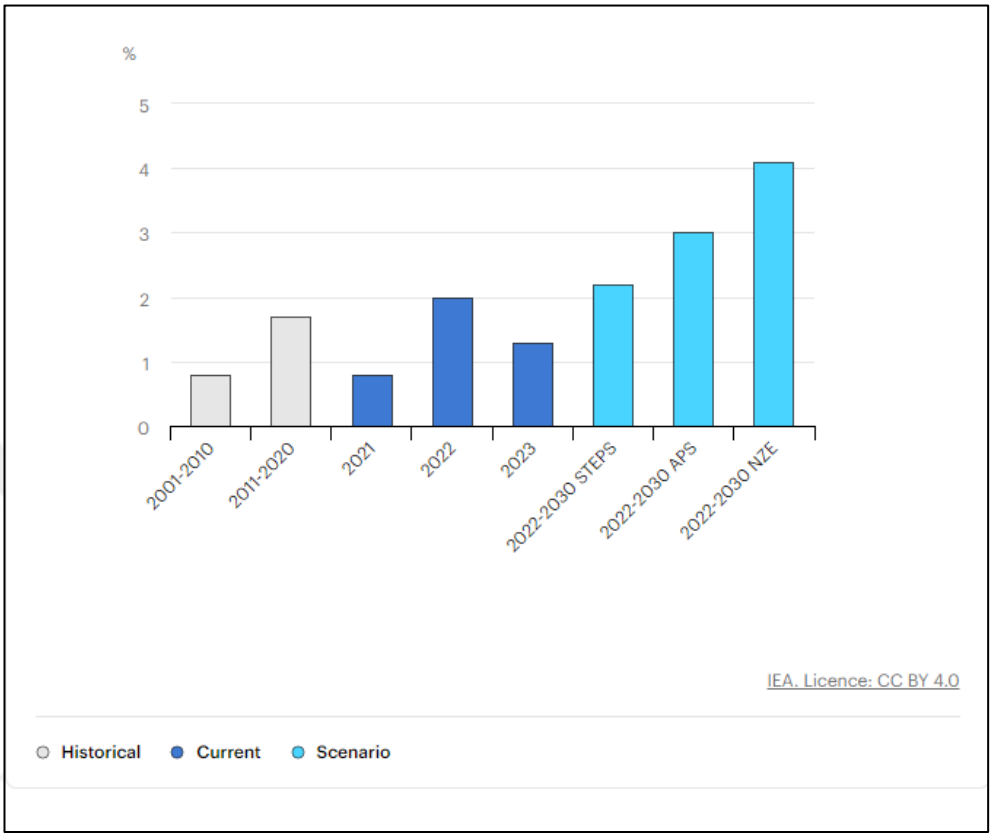

Figure 1.2 Energy efficiency trends over the years

So far, there has been no consistent increase or decrease in energy efficiency measurements. However, the highest energy efficiency was recorded around 2% in the year 2022 (IEA, 2023).

Due to such low energy efficiency, an excess of energy is being generated, and a significant amount of the produced energy is being released as waste, rendering it unusable.

A considerable amount of mechanical and electrical energy is lost as heat, primarily due to friction and resistance. Moreover, various industrial processes generate substantial amounts of unusable waste heat energy, which cannot be effectively harnessed for further use (Pradhan & Yadavalli, 2024). Therefore, increasing the

utilization of this excess energy and enhancing energy efficiency have become crucial. While the released heat energy can be utilized through heat transfer, converting excess heat into electricity could be a more practical method. This conversion is made possible through thermoelectric materials.

1.1. Thermoelectricity

Converting waste heat energy into electricity is a recognized and optimal approach. Thermoelectricity is the scientific field dedicated to the conversion between heat and electricity. Devices converting electricity to heat are termed Peltier modules, while those converting heat to electricity are known as thermoelectric generator (Li, 2023). The Seebeck effect, Peltier effect, and Thomson effect are the most crucial thermoelectric effects.

1.1.1. Seebeck Effect

The Seebeck effect describes the generation of a potential variation between two surfaces of a material due to temperature differances. When a heat difference is applied across two edges of a material with different conductivity characteristics, a potential difference arises between these points, as depicted in Figure 1.3. This potential difference is directly proportional to the heat transfer between the edges. Equation 1.1 provides the theoretical calculation formula for the generated electricity.

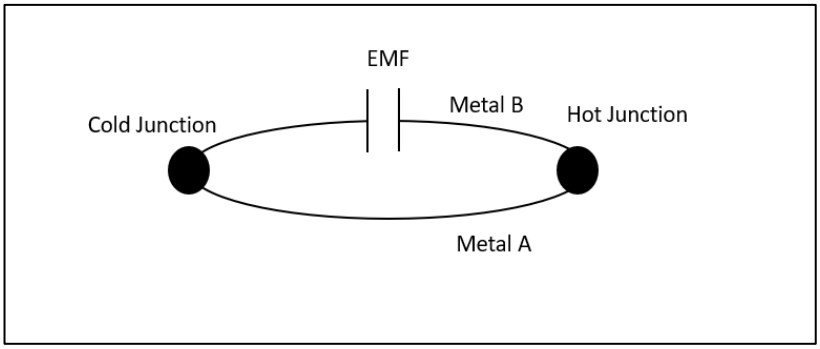

Figure 1.3 Seebeck Effect

$$\Delta V = S.\Delta T \quad (1.1)$$

ΔV is the potential difference, S Seebeck coefficient and ΔT is the temperature difference between Cold and Hot junction.

The Seebeck effect is described by the **Hata! Başvuru kaynağı bulunamadı.**
In the equation, E represents the potential change owing to the temperature difference, S represents the Seebeck coefficient, and ΔT indicates the temperature difference(Mammadov, et al., 2023).

1.1.2 Peltier Effect

The Peltier effect, discovered by Charles Peltier in 1834, occurs when DC current is applied to the contact points between two different semiconductors. While one side is cooled, heat is produced on the other side. The heat produced is directly proportional to the applied DC current (Figure 1.4)(Usta & Kirmaci, 2002).

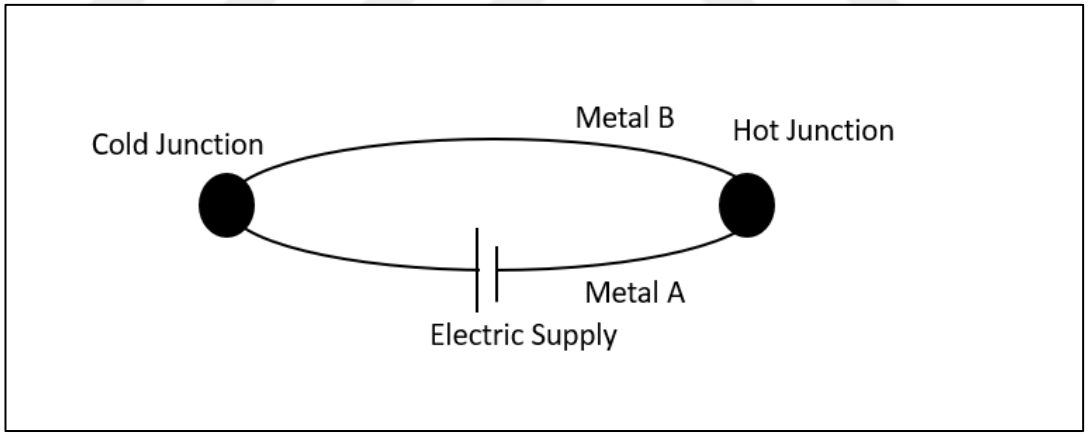

Figure 1.4 Peltier Effect

1.1.3. Thomson Effect

The Thomson effect, derived from the Seebeck and Peltier effects, was discovered approximately 20 years after those discoveries (Hüner, 2018). If there is a temperature

difference between any two points in a conductor through which current is passing, heat is absorbed or released depending on the applied current and the material of the conductor. This phenomenon is called the Thomson effect (Lee, 2013) and shown in Figure 1.5.

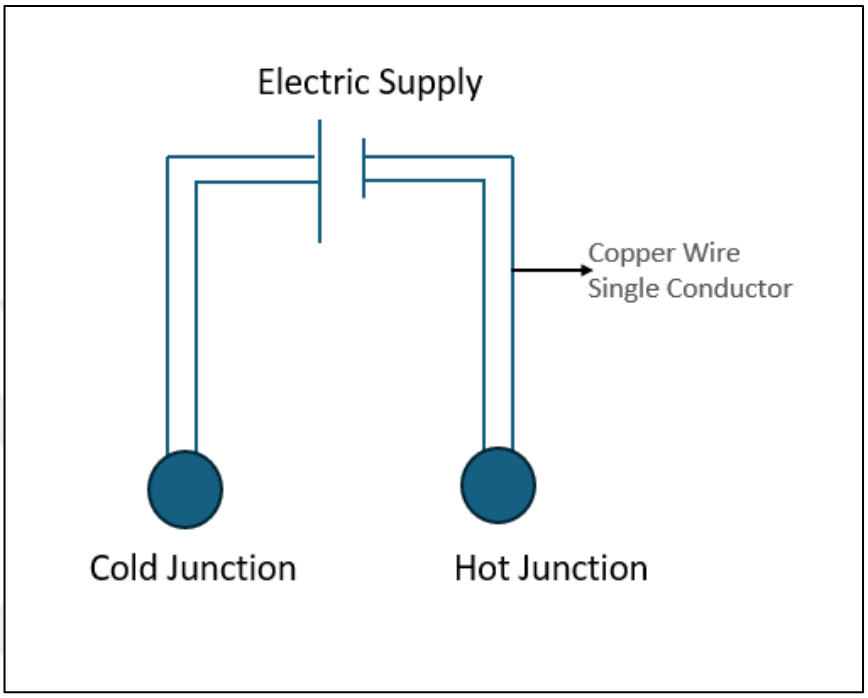

Figure 1.5 Thomson Effect

1.2 Thermoelectric Materials

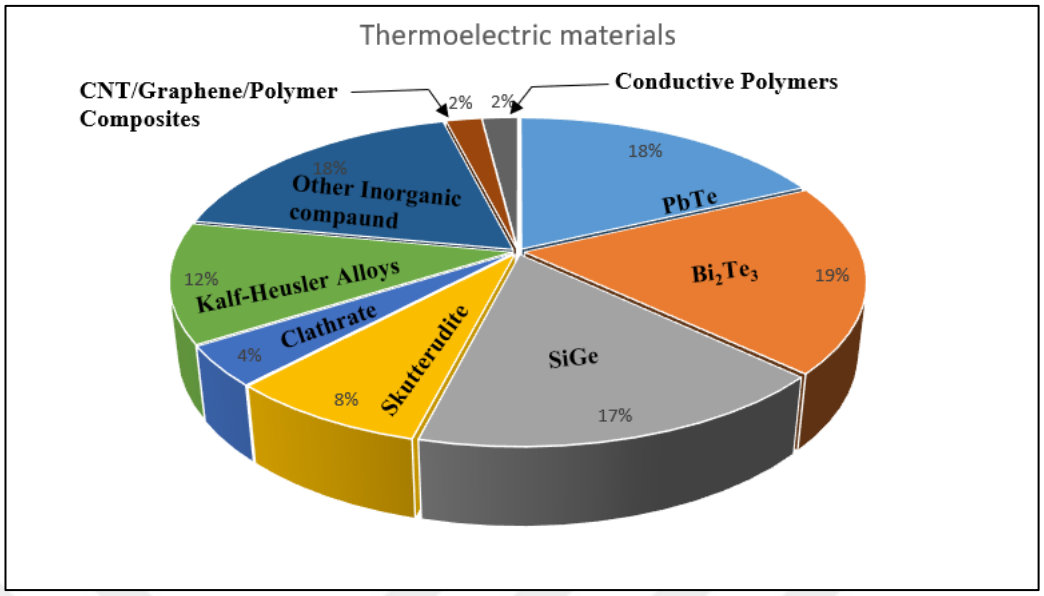

Figure 1.6 Usage rates of divers TE materials

In their 2019 study Yao et al. shared their findings on the new applications and developments of thermoelectric materials. In recent years, researchers' interest in polymeric thermoelectric materials has increased due to advantages such as low cost, physical flexibility, and ease of processing. Conductive polymers and carbon-polymer-based hybrid structures constitute 4% of the total thermoelectric materials (Figure 1.6) (Yao, et al., 2019).

Thermoelectric materials can be categorized into two groups based on the types of charge carriers they possess. These material are called P-type and N-type (Güldiken, 2011).

1.2.1 P-Type Materials

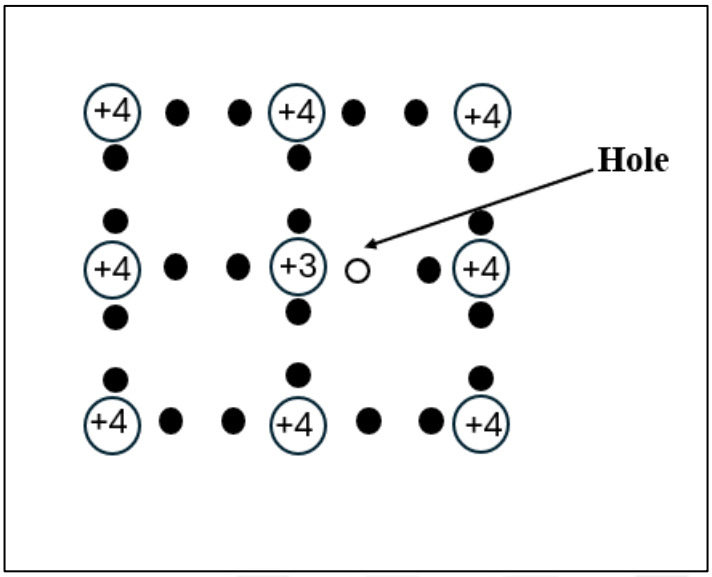

Figure 1.7 Schematic representation for P-type material

P-type materials are obtained by doping an atom with 3 valence electrons into a crystalline structure formed by atoms that have 4 valence electrons. Silicon and indium have 4 and 3 valence electrons respectively. When indium is introduced into the silicon crystalline lattice, it forms bonds with 3 silicon atoms, leaving the fourth silicon atom without a bond due to the lack of a valence electron in the indium atom. As a result, the fourth silicon atom is introduced with a hole instead of an electron. The formed hole can move through crystalline lattice by making the material conductive. Therefore, the electrical current flows through the material using these holes. The electrical conductivity of the material is directly dependent on the concentration of these holes. These materials are known as P-type, where holes are the primary charge carriers and electrons are the secondary charge carriers (Figure 1.7).

1.2.2 N-Type Materials

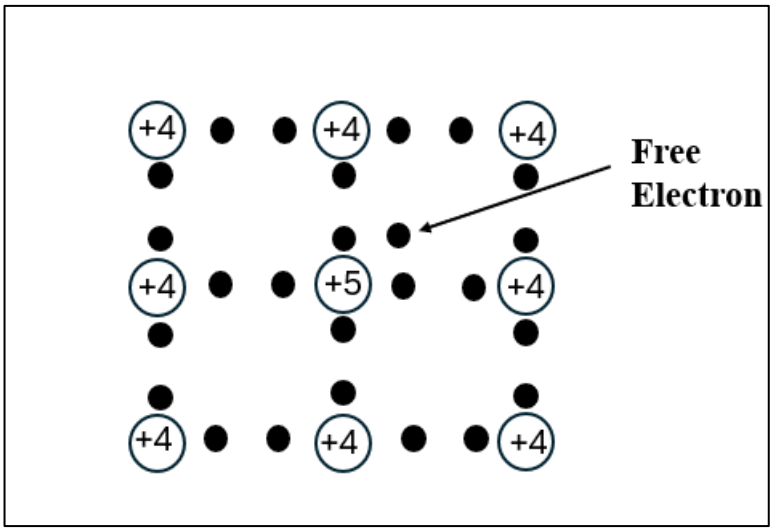

Figure 1.8 Schematic representation for N-type material

N-type materials are mostly the opposite of P-type materials, they can be prepared by introducing an atom with 5 valence electrons into chemical structure that is formed by atoms with 4 valance electrons. Antimony contains 5 valance electrons therefore it can bond with 4 silicium atoms and add an extra electron into material's structure. These types of semiconductors are known as N-type materials where electrons are the primary charge carriers (Figure 1.8). Conductivity of the material is directly related to the free electron intensity (Derebaşı, 2015).

1.3 Polymers

The word "polymer" was first coined by the Swedish scientist J.J. Berzelius. In this term, "poly-" means many, while "-mer" signifies parts(Feldman 2008). Simply put, polymers, meaning multiple parts, are formed by the chemical bonding of numerous monomers with each other. Polymer chemistry, which can be considered a relatively new field in chemistry, began to be enlightened with Hermann Stadudinger's Nobel Prize-winning work in 1953. Polymers can be divided into two main classes: natural (such as cellulose, lignin, starch, etc.) and synthetic (such as polyethylene, polypropylene, polyvinyl chloride, etc.).

The number of monomers in the polymeric structure could have a significant effect on the polymers' physical properties. This number is referred to as the degree of and

represented by ‘‘*n*’’. It is possible to obtain polymers that are chemically similar but have different applications by only changing the *n*. The properties of polymers can vary in many aspects and a short list of these can be listed as follows:

- Polymerization degree (*n*)
- Chemical structure of the monomer
- Chemical interactions between polymer chains
- Chemical bonds in between polymer chains (cross linking) (Vahapoğlu, 2013)

In addition to their vast chemical properties, polymers can also undergo modification through several methods. These modifications could alter their characteristic properties such as mechanical properties, thermal properties, conductivity, chemical resistance (Hudson, 2018).

1.3.1 Electrical Conductivity in Polymers

Conductivity of a materials is generally dependent on the energy levels of their valance band and conductive band. The energy differential between these bands determines a material’s electrical conductivity characteristics. When energy is applied to a material equal to the energy differential between bands.

- If the material alters its chemical structure, it could be insulating material.
- If the material maintains its chemical structure and becomes conductive, it could be semiconductor.
- If the material does not change any chemical or physical property and directly transmits it through itself, material could possibly be conductor.

A schematic presentation of the conductive and valance band for conductive, semiconductive and insulator materials is given in Figure 1.9.

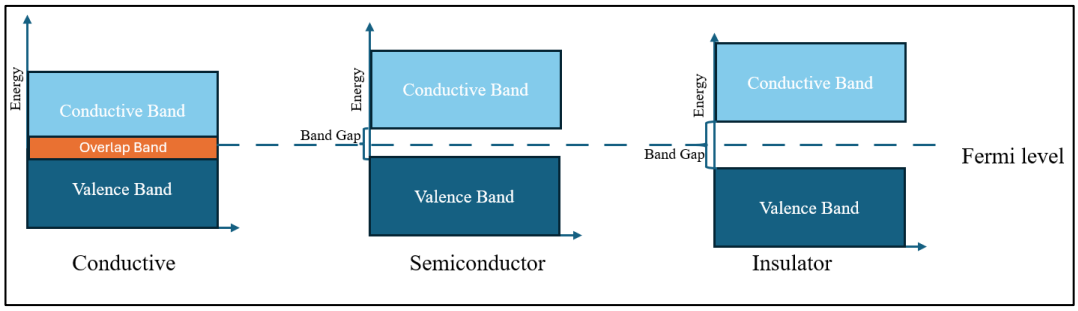

Figure 1.9 Band gap for conductive, semiconductor and insulator materials

1.3.1.1 Insulating Polymers

When the energy applied to materials equal to its energy difference in between valance and conductive bands if material changes its chemical structure or undergo reaction the material is generally an insulator (Aydin, 2012). Polyethylene terephthalate, polymethyl methacrylate, and polydimethylsiloxane can be cited as examples of insulating polymers. Even though there are currently several semiconductor and conductor types of polymers, they were known as insulating materials until polymers with conjugated bonds were discovered (Mutlu et al., 2023).

1.3.1.2 Semi-conductor Polymers

Supplying energy to semiconductor polymers equals the energy difference between valance and conductive bands allows electrons to move to the conduction band. These electrons then freely conduct electric current within the material, leaving behind a gap as they move. When the supplied energy is removed, the electrons return to fill the gap, and the material reverts to being an insulator. It is possible to modify polymers such as polyacetylene and polypyrrole to create semiconductor materials, thereby increasing their conductivity. In silicone-based polymers, semiconductor properties can be achieved by attaching additional organic structures to silicone atoms. These modifications can enhance or adjust the electrical conductivity of silicone polymers. These methods play an important role in promoting the use of semiconductor polymers in electronic devices, sensors, solar cells, and other electronic applications (Özbağ, 2010).

1.3.1.3 Conductive Polymers

Conductive polymers are materials that provide electrical conductivity through double bonds in their structures, while also possessing flexible and processable properties. For example, organic polymers such as polyacetylene, polypyrrole, polyaniline, and polythiophene can achieve high levels of conductivity by increasing the number of electron carriers (Nezakati et al., 2018).

1.3.1.3.1 Polyacetylene

After one of the π bonds of acetylene (H−C≡C−H) is broken, the resulting radical (-CH=CH-) molecules react with each other to form polyacetylene. Polyacetylene, which has sp2 hybridization, can be synthesized in different isomeric structures, namely cis and trans forms (Gaurav et. al. 2021; Özbağ, 2010). When Ti[O(C4H9)]4 /Al(C2H5)3 is used as a catalyst in the polymerization reaction, cis-polyacetylene is obtained, while trans-polyacetylene is obtained when n-hexadecane is used. It possesses a linear and conjugated structure, and it can easily undergo oxidation reactions with oxygen through its double bonds. The structures of cis and trans isomers are depicted in Figure 1.10 (Özbağ, 2010).

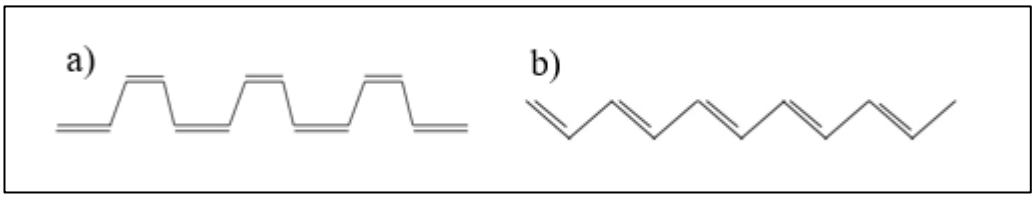

Figure 1.10 a) Cis-polyacetylene b) Trans-polyacetylene

1.3.1.3.2 Polypyrrole

Polypyrrole (Figure 1.11) is a highly flexible material with a higher density (1.6 g/cm3) compared to other conductive polymers. One of the most common synthesis methods for polypyrrole is the electrochemical method. When an appropriate potential difference is applied to a system consisting of an electrolyte solution containing pyrrole molecules and a working electrode, pyrrole molecules are oxidized on the electrode surface, forming radical cations. These radicals then react with each other to

produce polypyrrole (Kaya, 2021). Polypyrrole is among the conductive polymers that can be stored for long periods while maintaining its usability (Zarei et al., 2021).

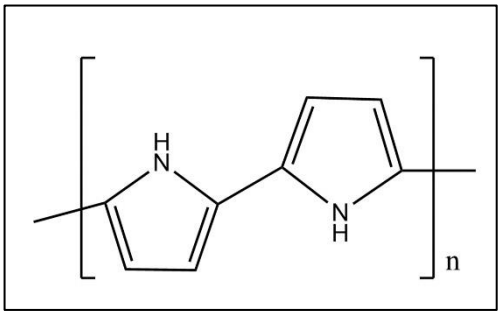

Figure 1.11 Polypyrole

1.3.1.3.3 Polyaniline

Due to its affordable starting material and adaptability to modification, polyaniline (Figure 1.12) has a wide range of applications (Kazemi et al., 2021). The aniline monomer reacts with a peroxide-based oxidizing agent to form radical cations. These cations then bond with each other to create a linear polymer chain (Boeva ve Sergeyev 2014). The $-NH_2$ groups on polyaniline become $-NH_3^+$ in an acidic environment, and this form of the polymer is called "emeraldine" (Bednarczyk et al., 2021).

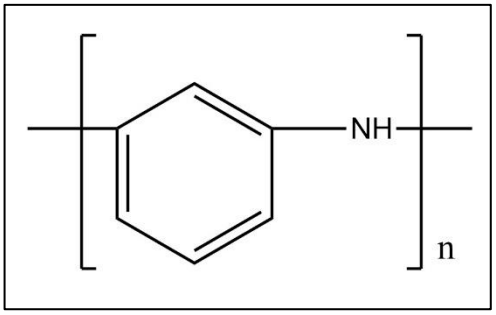

Figure 1.12 Polyaniline

1.3.1.3.4 Polythiophene

It is a conductive polymer with a sulfur heterocycle. Thiophene rings become cationic radicals when they reduce Fe^{+3} ions to Fe^{+2} ions, leading to the formation of the polymeric structure (Patil, et al., 2012). It is a thermally, environmentally, and chemically resistant polymer (Husain et al., 2023; Sasaki et al., 2021). Despite these advantages, its low solubility is one of its major drawbacks. To overcome this disadvantage, polythiophene (Figure 1.13) can be modified to become soluble.

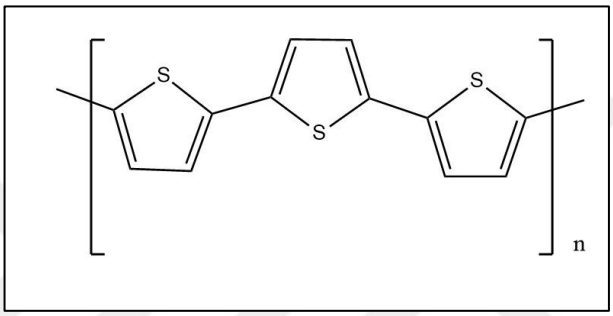

Figure 1.13 Polythiophene

- ***Poly(3,4-ethylenedioxythiophene) polystyrene sulfonate***

PEDOT is a thiophene derivative polymer with a stable structure that exhibits similar characteristics to semiconductors with regard to electrical conductivity and the energy gap between the valence and conduction bands (Wang, 2009). PEDOT is a polymer with low solubility in water, and to increase its solubility, PSS is added to the environment during the synthesis of PEDOT. PSS, being anionic, creates an electrostatic attraction with the positively charged portion of PEDOT's backbone, thereby enhancing PEDOT's solubility. This process results in PEDOT transitioning to the PEDOT:PSS form, which increases solubility while reducing electrical conductivity (Liu et al., 2015; Pinto et al., 2023; Zhang, et al., 2005). Although PEDOT:PSS (Figure 1.14) maintains a certain level of electrical conductivity, factors such as the solvent, additives, and the amount and type of additive (DMSO, EG, PEG, etc.) directly influence the electrical conductivity of the matrix within the solvent (Crispin et al., 2003; Horii et al., 2018; Jönsson et al., 2003).

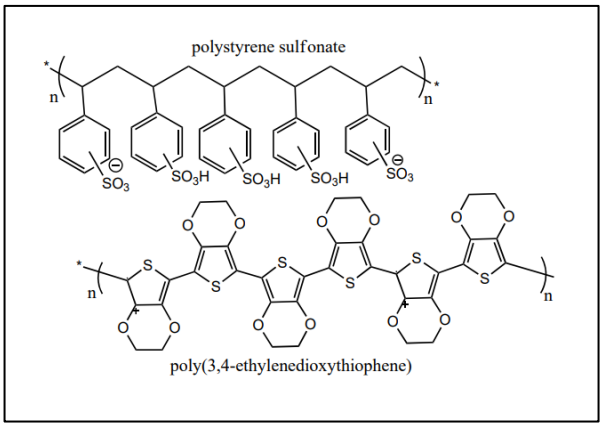

Figure 1.14 Poly(3,4-etylenedioxythiophene)-Polystyrene sulfonate

- ***Application of PEDOT: PSS***

Due to its ease of processing, suitable electrical and thermal conductivity, and transparency, PEDOT:PSS has become a widely used polymer in thermoelectric applications (Feng, et al.,2020). It is also extensively utilized in electronic device applications and has garnered significant interest. PEDOT:PSS, along with various additives, has been commonly used in solar panels (Wan et al., 2021), supercapacitors (Su et al., 2022), electronic textile products (Alshabouna et al., 2022) and tissue engineering (Xu et al., 2021).

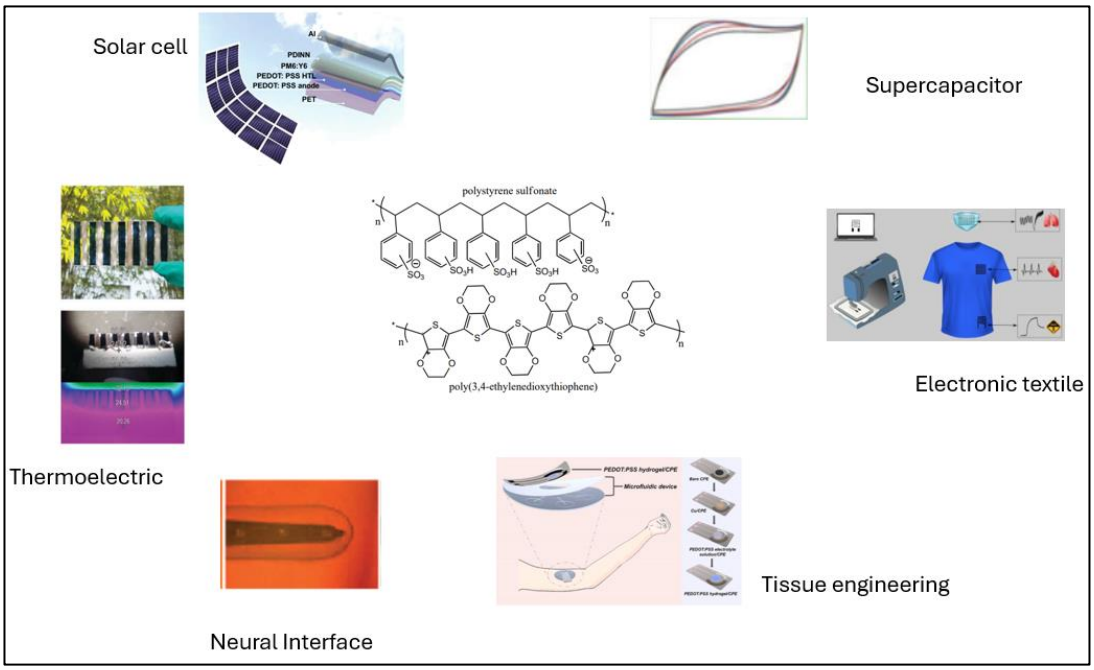

Figure 1.15 Usage area of PEDOT: PSS

Due to its non-toxic nature, PEDOT: PSS has also found its place in biological applications. Some of these applications include; sensors for biomedical applications (Pradhan & Yadavalli 2024), organic electrochemical devices for bio-sensing, and transistors (Huang et al., 2024; Liang, et al., 2018) as well as nerve interfaces (Green & Abidian, 2015; Han et al., 2022) (Figure 1.15).

CHAPTER TWO
PREVIOUS STUDIES

Increasing the efficiency of systems due to the increasing energy need and ensuring the recovery of this energy by utilizing the waste heat in these systems are among the popular topics (Shi, et al., 2020). Thermoelectricity stands out among the intensively studied topics in energy harvesting. In thermoelectricity, studies with traditional inorganic materials are being replaced by organic polymer-based modules. In this way, materials can be more affordable, easily processed and have flexible structures. From these perspectives, thiophene-based PEDOT: PSS is frequently used in thermoelectric applications. From these perspectives, thiophene-based PEDOT: PSS is frequently used in thermoelectric applications. In studies conducted for this purpose, Lu and his colleagues prepare high-performance pure PEDOT: PSS hydrogels, which they conducted in 2019. Drying and annealing process is performed by adding different ratios of DMSO into aqueous PEDOT: PSS. DMSO added at a rate of 13% exhibits the highest electrical conductivity with nearly 20 S/cm in PBS and 40 S/cm in distilled water (Lu, et al., 2019) . In addition, Xin et al. reported in 2019 in their studies, they investigated the effects of freeze drying and heat drying on the mixtures to be prepared afterwards. In this study, mixtures were prepared by adding 5% DMSO by weight into PEDOT: PSS, which was prepared by lyophilization and dried with the help of an oven. While it is observed that films prepared by freezing heal themselves and work with the same performance after days, it is seen that films prepared with the help of an oven cannot self-heal themselves (Xin, et al., 2019). After this study, with the increasing effect of layered production technology, Yuk and his colleagues published their work titled '3D printing of conducting polymers' in 2020; They prepared inks containing high amounts of PEDOT: PSS and examined the performance of these inks. They obtained nanofibrils by lyophilizing the aqueous PEDOT: PSS solution. Then, the obtained PEDOT: PSS was added to the DMSO/Water mixture, which is a binary solvent mixture. While the electrical conductivity of the inks prepared for the 3D printer in their dried state was 155 S/cm, the electrical conductivity of the inks in hydrogel form was measured as 28 S/cm (Yuk, et al., 2020). In the study titled 'Facile material extrusion of 3D wearable conductive-polymer micro-super-capacitors' conducted by Li et al. in 2023, they prepared PEDOT: PSS mixtures with different

ratios and made super micro capacitors with the help of a 3D printer. In this study, contrary to the literature, PEDOT: PSS was dried by impregnation with a superabsorbent polymer. Afterwards, the mixture was prepared by adding DMSO in different proportions to create ink. According to the results obtained, excessive use of DMSO added to the mixture reduces the viscosity and increases the electrical conductivity (Li, et al., 2023).

As the importance of PEDOT: PSS has escalated over time, researchers have explored the effects of incorporating different materials into its matrix. The effects of incorporating multi-walled carbon nanotubes (MWCNT) into PEDOT: PSS on its characteristics were investigated in a 2016 study by Benchiriuf et al. From 0.025% to 0.1% by weight, they experimented with different concentrations of MWCNT and used these mixes to create thin films. They then put these films through tests in a range of temperatures and humidity conditions. Their findings showed that the films' resistance to electricity increased with increasing humidity. On the other hand, resistance decreased as temperature rose. This indicates that the environment can have an impact on these nanocomposite films' electrical activity (Benchirouf, et al.,2016). In their 2017 investigation, Liu et al. synthesized PEDOT: PSS from EDOT and introduced graphene and MWCNT into the polymer matrix. Within the scope of this study, the electrical conductivity, Seebeck coefficient, and PF (power factor) values were determined at ambient temperature, yielding 2.936 S/cm, 18.9 μV/K, and 0.105 $\mu W/mK^2$, respectively(Liu et al., 2017). After this investigation, Mannayil and colleague undertook a study employing functionalized multi-walled carbon nanotubes (f-MWCNTs). They fabricated films from PEDOT: PSS/f-MWCNT solutions using the Spin-Coating technique. Remarkably, the electrical conductivity of the film containing 0.3% f-MWCNT was measured at 1 S/cm, while the film incorporating 2% MWCNT exhibited an electrical conductivity of approximately 20 S/cm. These findings underscore the pronounced influence of MWCNT concentration on the electrical characteristics of PEDOT: PSS-based films (Mannayil, et al.,2018).

Liu et al. (2019), graphene/PEDOT: PSS nanocomposite films were utilized for the fabrication of flexible thermoelectric power generators. Graphene was incorporated

into the PEDOT: PSS matrix and films were prepared using the vacuum filtration technique. According to the obtained results, the electrical conductivity of the prepared films was measured at 1016.5 S/cm, with a Seebeck coefficient of 15.5 μV/K (Liu et al., 2019).

Additionally, studies involving the addition of inorganic materials alongside carbon-based materials have been conducted. In a study conducted by Park et al., Ag_2Se nanowires were synthesized and subsequently incorporated into PEDOT: PSS. The electrical conductivity of the films prepared using the drop-casting method was found to be inversely proportional to the Ag_2Se content; as the Ag_2Se content increased, the electrical conductivity decreased. However, the results of the Seebeck coefficient indicated a transition from p-type to n-type characteristics in films containing 20% Ag_2Se. This suggests that the addition of Ag_2Se alters the thermoelectric properties of the film, exhibiting n-type characteristic features (Park, et al., 2020).

In various studies, it has been observed that the electrical conductivity of commercially used PEDOT: PSS aqueous solution or PEDOT: PSS obtained as a result of polymerization is insufficient. The electrical conductivity of PEDOT: PSS increases when used with carbon-based materials. For this reason, in some studies, the Seebeck coefficient and electrical conductivity were examined using a mixture of PEDOT: PSS and carbon-based materials, and it was determined that this mixture increased its electrical conductivity and also showed P-type material properties.

Within the scope of this study, 1-1.3% commercially purchased PEDOT: PSS was lyophilized to increase the polymer ratio in the mixture and with this increase, it was aimed to increase the electrical conductivity. At the same time, the effects of adding carbon-based materials on the electrical conductivity of the material were examined. N-type characteristics were examined by adding Ag_2Se to this mixture, which showed P-type material properties.

CHAPTER THREE
MATERIALS AND METHOD

3.1 Materials

Poly(3,4-ethylenedioxythiophene) polystyrene sulfonate (PEDOT: PSS), (product ID: 483095) containing 0.8 wt.% PSS, and 0,5% Pedot was obtained from Sigma Aldrich. Dimethyl sulfoxide (DMSO) from Carlo Erba was chosen to promote the dispersion of PEDOT: PSS. Graphene nanoplatelets (7 µm diameter, 5 nm thickness) and Multi-Walled Carbon Nanotubes (CNTMWs) with a diameter below 8 nm were sourced from Nanography. Additionally, Ag_2Se (ID: 400637) was purchased from Sigma Aldrich, and Sorbitol (Lot: 120220826) from Smart Chemical Company.

3.2 Method

Selecting the substrate is one of the most crucial steps in the film preparation process. Mistakes made during material selection can result in the film not adhering to the substrate or failing to form a film.

Additionally, there's a risk of the material excessively drying out, volatile components evaporating from within the film, and conductivity measurements being adversely affected. For this reason, the optimum film preparation parameters were determined before starting the parameter studies. During preliminary trials, we considered factors like substrate type, ideal film thickness, and drying temperature to ensure the film's removal from the surface without deformation. Homogenization trials, tailored to the type of additive used, aimed to attain the ideal homogenization of the solution for the film-making process.

3.2.1 Pre-production trials for film formation

3.2.1.1 Substrate test

In the experiments, a commercially purchased aqueous solution which includes 1.0–1.3% PEDOT: PSS was used. It was mechanically stirred for six hours before being filtered via a syringe filter. Following that went through a pre-lyophilization stage that involved 12 hours of freezing at -20°C. After that, it was purified for three days at 1.0 mbar pressure and -51°C. These processes resulted in the formation of a sponge-like structure of PEDOT: PSS polymer (Figure 3.1).

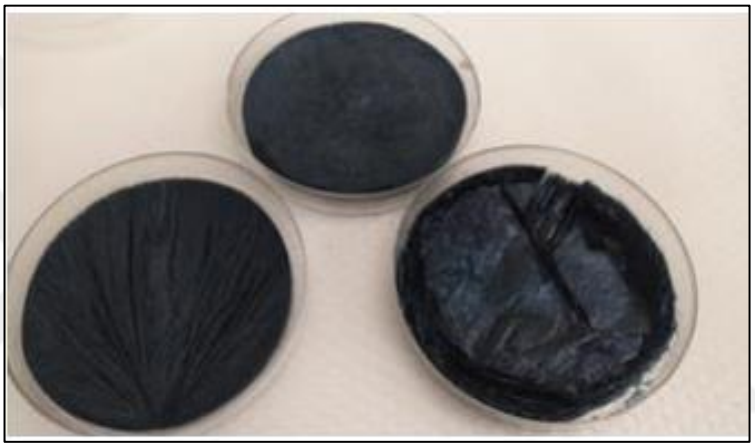

Figure 3.1 After the lyophilization PEDOT: PSS polymer (Personal archive, 2022)

Solutions were prepared by adding PEDOT: PSS at 3-5% and 7% by weight to a mixture of 15/85 (v/v) DMSO-water. These solutions (Figure 3.2) were stored at +4°C before film preparation for characterization.

Figure 3.2 PEDOT: PSS solution (Personal archive, 2022)

It is necessary to have a substrate for film preparation. Here, three distinct substrate choices were selected: Teflon, Parafilm, and mirror (respectively). Before film preparation, surface cleaning used acetone and alcohol. Subsequently, films with a thickness of 50 microns were prepared using a doctor blade, which serves as a film preparation applicator.

Figure 3.3 PEDOT: PSS films (50 micron) (Personal archive, 2022)

The prepared films were exposed to 60°C for 24 hours. At the end of the first day, they were annealed by being held at 130°C for 30 minutes in three cycles. After every 30-minute interval, the films were removed from the oven and allowed to cool to laboratory conditions before proceeding to the next cycle. Films prepared after three cycles are shown in Figure 3.3. On the Teflon and Parafilm substrates, a perfect film was not formed, but the dried substance was still easily removed from the surface. On the mirror surface, an ideal film was created, however it was difficult to separate from the surface.

3.2.1.2 Film thickness

Experiments were conducted with various film thicknesses to find substrates with surfaces that are hydrophilic enough to allow the spread of the prepared solution to form a film yet hydrophobic enough to facilitate the detachment of the film from the surface.

The substrate materials used were PVC (Poly Vinyl Chloride), heat-treated PVC, PP (poly propylene), PC (polycarbonate), and PDMS (Polydimethylsiloxane) (Figure 3.4).

Figure 3.4 PEDOT: PSS film (100 micron) (Personal archive, 2022)

As a result of the experiments, ideal film formation was observed on all substrates. Despite varying the thickness of the prepared films, they remained firmly attached to all surfaces without undergoing any deformation.

3.2.2.1 Drying experiments

Drying experiments were conducted using five diverse substrates: polypropylene, polyethylene terephthalate (PET), PVC, aluminum foil, and acetate paper. Vacuum drying was attempted; however, after 2 hours, deformation occurred in the films. Therefore, vacuum drying was not pursued.

The prepared films in this experimental setup were allowed to dry at the room temperature, 60°C, 90°C, and 120°C. It was found that as the temperature increased, fractures emerged on the surface of the oven-dried films, which did not separate from any surface. After a day of drying, films made at room temperature had minimal surface deformation and were effortlessly removed from all surfaces. The best surfaces were found to be PP and PC. Preliminary investigations revealed that drying temperature has a greater influence on the production of an ideal film than film thickness and surface.

3.2.2 Homogenization experiment

Homogenization studies were conducted in parallel with the film formation preliminary experiments.

3.2.3.1 Carbon additive trials

0.5% graphene was added to a DMSO/Water mixture containing 5% PEDOT: PSS. Afterward, the resulting mixture was vigorously stirred on a magnetic mixer for 1 hour. Afterward, the mixture was poured onto a suitable substrate to form a film (Figure 3.5a).It was left to dry at room temperature for 24 hours (Figure 3.5b). It was observed that the mixture prepared in both methods was not adequately homogenized.

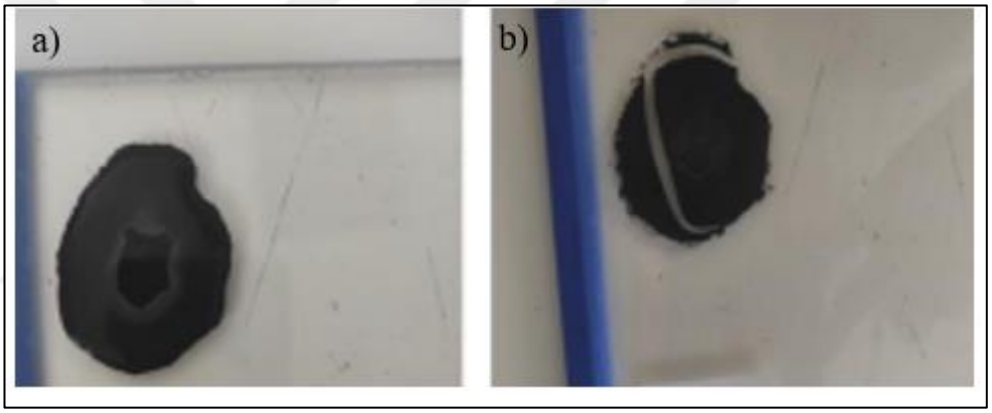

Figure 3.5 PEDOT: PSS /GR film a) wet b) dry (Personal archive, 2022)

The mixing method used by Pillai et al. (Pillai, et al., 2021) involved subjecting the solution to 60 minutes of ultrasonic mixing followed by 30 minutes of exposure to a magnetic stirrer. After four cycles, the solution was further mixed on a magnetic stirrer for 72 hours. Carbon-based materials were mixed and transformed into films using this mixing cycle (Figure 3.6).

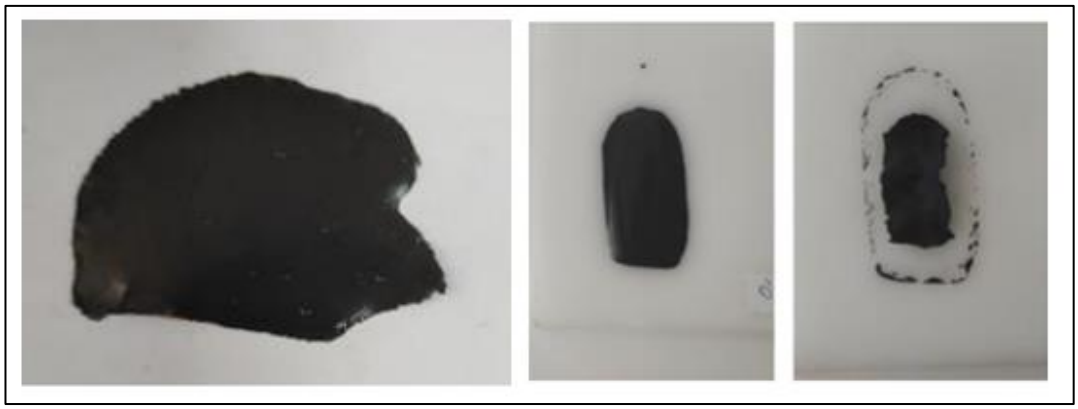

Figure 3.6 PEDOT: PSS /CNTMW films (Personal archive, 2022)

After separately preparing each carbon-based material, efforts were made to mix both materials. These carbon-based compounds were mixed using the same procedure, with the weight proportions of 0.25% graphene and 0.25% CNTMW determined. Subsequently, films were prepared and left to dry at room temperature.

Although the total carbon material content of the prepared film was 0.5%, there was no clumping observed in the solution, and no moire were visible on the surface of the film after preparation (Figure 3.7)

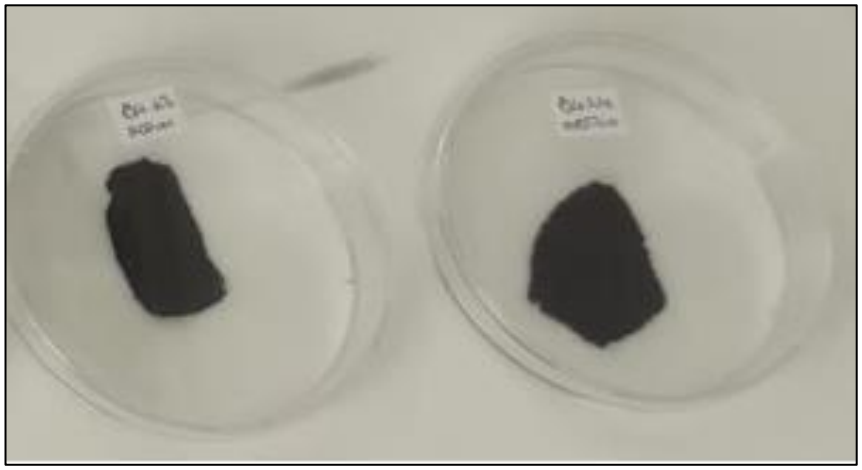

Figure 3.7 PEDOT: PSS/CNTMW/GR films (Personal archive, 2022)

The mixing technique that Pillai et al. have recommended will be applied in this instance. Consequently, the conditions for mixing will be an ultrasonic bath for 60 minutes, followed by 30 minutes of mixing on a magnetic stirrer for four cycles.

Following these procedures, the solution placed on the magnetic stirrer for 72 hours will become a film.

3.2.2.2 Preliminary studies of $CuCl_2$

Under argon gas, a solution containing 5% PEDOT: PSS was stirred for 5 minutes. Then, 10% $CuCl_2$ by weight was added, and the mixture was stirred for an additional 60 minutes to form a film (Figure 3.8 a and b). As seen in Figure 3.8, the resulting film does not have a homogeneous structure. That is due to the insufficient dissolution of the solid $CuCl_2$ within the dense 5% PEDOT: PSS solution.

Based on the information obtained, $CuCl_2$ was first dissolved in the DMSO/water mixture, followed by the incorporation of PEDOT: PSS at a weight percentage of 5%. The blend was vigorously stirred on a magnetic mixer under argon gas for 1 hour. The resulting mixture was then prepared to form a film as depicted in Figure 3.8 c and Figure 3.8 d.

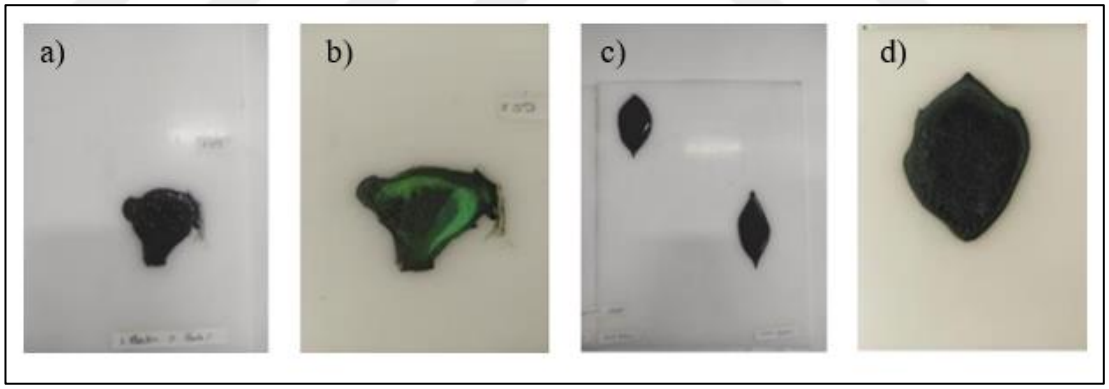

Figure 3.8 5% PEDOT: PSS/ 10% $CuCl_2$ content films (Personal archive, 2022)

Even though the produced films were homogeneous, it was noted that after drying, they became intensely fragile. The films were manufactured once more after the $CuCl_2$ additive ratio was lowered from 10% by weight to 2.5% to address the fragility issue. Figure 3.9 displays mixtures containing 2.5% by weight of $CuCl_2$ solid.

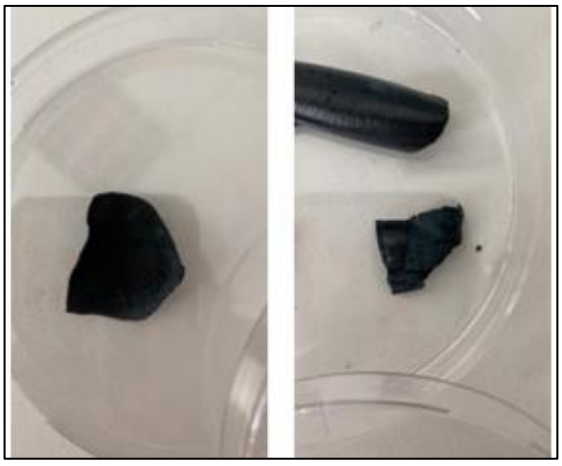

Figure 3.9 5% PEDOT: PSS/ 2.5% $CuCl_2$ content films (Personal archive, 2022)

Since reducing the $CuCl_2$ ratio did not resolve the fragility issue in the films, Sorbitol, also known as a plasticizer, was added to the formula, and the films were prepared again (He & Ouyang, 2020). The obtained mixture was transformed into films using the drop-cast method. The prepared films were dried at room temperature. The resulting films can be seen in Figure 3.10.

Figure 3.10 PEDOT: PSS/$CuCl_2$/SORBITOL films (Personal archive, 2022)

Even with the addition of a plasticizer, the films created by this technique stayed adhered to the substrate and showed fragility. It was not possible to examine the impact of $CuCl_2$ in this study because neither measurements nor films were made during the investigation.

3.2.2.3 Preliminary studies of Ag_2Se

A mixture containing 10% Ag_2Se was added to a solution of 5% PEDOT: PSS and mixed for 60 minutes using ultrasonication followed by 30 minutes on a magnetic stirrer for four cycles. Subsequently, it was further mixed on a magnetic stirrer for 72 hours. However, as seen in Figure 3.11 a, the mixture reached a paste-like consistency, and a film was prepared from this material (Figure 3.11 b).

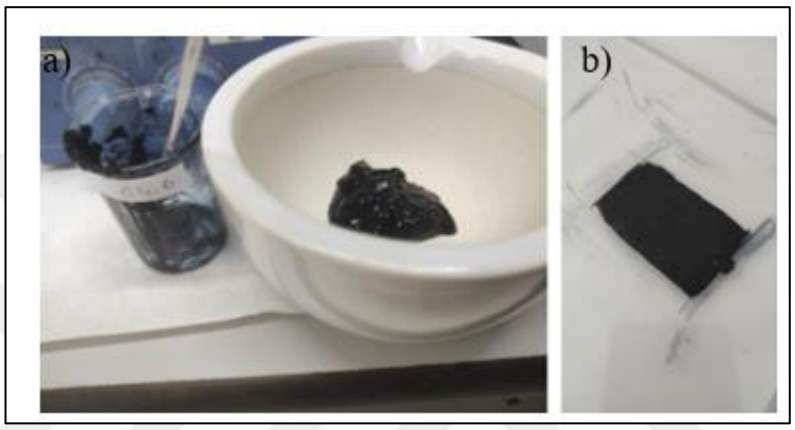

Figure 3.11 5% PEDOT: PSS/ 10% Ag_2Se solution and film (Personal archive, 2022)

Upon air drying at room temperature, the film developed cracks. In light of the mixture's density and the presence of cracks, the Ag_2Se ratio was reduced to 5% to proceed with the experiments. Nevertheless, it was observed that the film structure remained fragile.

Based on the study conducted by Park et al., further mixing, and drying experiments were carried out (Park, et al., 2020).

A commercially purchased PEDOT: PSS solution containing 1-1.3% PEDOT: PSS was mixed with 5% DMSO in an ultrasonic bath for 30 minutes. Subsequently, 2.5% Ag_2Se by weight was added to this mixture and left in the ultrasonic bath for 3 hours. As a result of these processes, a film was prepared using the Drop-Cast method and left to dry at room temperature on two different surfaces (PP and silicone base) (Figure 3.12).

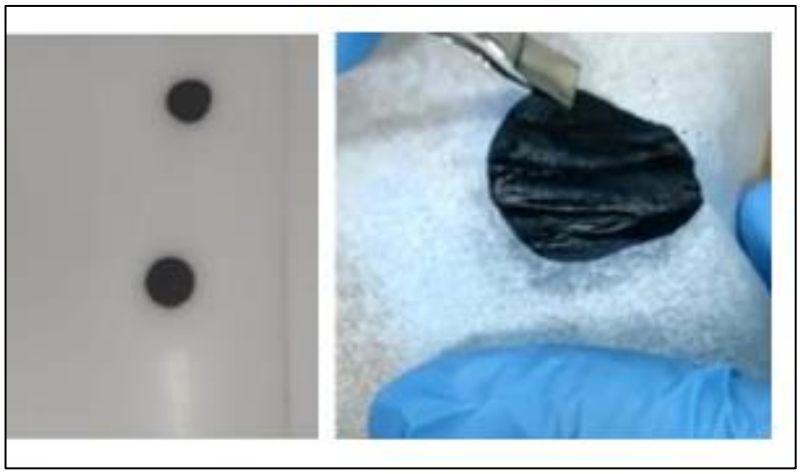

Figure 3.12 PEDOT: PSS/ 2.5% Ag_2Se content films (Personal archive, 2022)

Throughout the experiments, a silicone-based substrate was preferred due to the film's inability to be removed after drying on PP. It was preferred to conduct studies with this addition on silicon-based substrates because the film that developed on PP could not remove. Experiments were carried out by raising the Ag_2Se ratio since Ag_2Se of 20% or more could be added to the mixture and make the material N-type.

After drying, the prepared films exhibited solidification of the Ag_2Se particles, with the PEDOT: PSS polymer forming a separate layer on top. That is thought to be due to the Ag_2Se solid having large particles (Figure 3.14).

Figure 3.13 a) PEDOT: PSS/20% Ag_2Se b) PEDOT: PSS/60% Ag_2Se films (Personal archive, 2022)

A plasticizer substance was added to stop the films from forming distinct layers. Furthermore, the mixture was supplemented with sorbitol, which is regarded as an effective film filler material (Hou et al., 2023), and films were created. As seen in Figure 3.14, films with 60% Ag_2Se additive were first added with 5% sorbitol by weight. It was noted that the Ag_2Se particles in the produced films dried without splitting into two distinct layers with the PEDOT: PSS polymer.

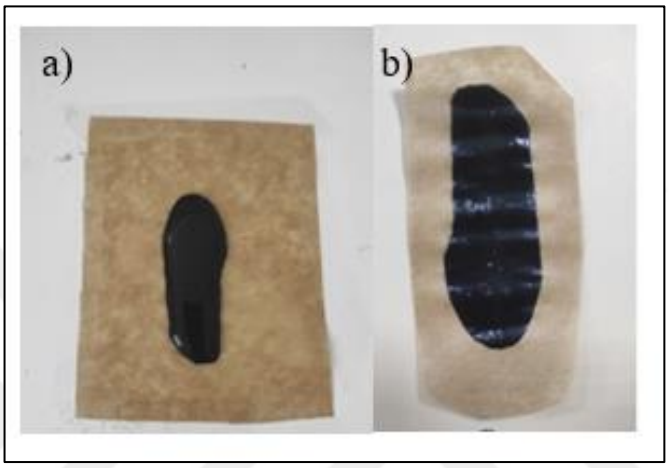

Figure 3.14 PEDOT: PSS/60% Ag_2Se a) wet b) dry (Personal archive, 2022)

All the early trials led to the identification of the best mixing techniques for each kind of additive. Moreover, ideal substrates were found to guarantee that ideal film's creation. Considering these results, a total of eighteen materials—P-type and N-type materials—were created to ascertain the impact of additions on electrical conductivity and Seebeck coefficient.

3.3 Studies using the Taguchi method

During the preliminary experiments, problems arose regarding the densification of the solution and the homogeneous distribution of other materials within the solution as the PEDOT:PSS ratio increased. Therefore, PEDOT:PSS ratios in the solution were adjusted to be 1-2% and 3%. The ratios of carbon-based materials to be added to the films were set at 0-0.25% and 0.5%. To distinguish between P-type and N-type materials in the films, Ag_2Se additives were adjusted to be 0-5-10-20-30 and 40% by weight. To prevent negative physical effects such as layering and cracking in the films due to the increase in additive ratios, 5% sorbitol was added to all mixtures. Due to the

numerous additives and their ratios, the Taguchi method was used to save on the number of experiments and materials used. The experimental design prepared using this method is provided in Table 3.1 and Table 3.2.

Table 3.1 Proportions of P-type material prepared by Taguchi method

P-Type Material	PEDOT: PSS (%)	Graphene (%)	CNTMW (%)	Ag_2Se (%)	Sorbitol (%)
Ppp1	1	0	0	0	5
Ppp2	1	0.25	0.25	5	5
Ppp3	1	0.5	0.5	10	5
Ppp4	2	0	0.25	10	5
Ppp5	2	0.25	0.5	0	5
Ppp6	2	0.5	0	5	5
Ppp7	3	0	0.5	5	5
Ppp8	3	0.25	0	10	5
Ppp9	3	0.5	0.25	0	5

Table 3.2 Proportions of N-type material prepared by Taguchi method

N-type Material	PEDOT: PSS (%)	Graphene (%)	CNTMW (%)	Ag_2Se (%)	Sorbitol (%)
Ppn1	1	0	0	20	5
Ppn2	1	0.25	0.25	30	5
Ppn3	1	0.5	0.5	40	5
Ppn4	2	0	0.25	40	5
Ppn5	2	0.25	0.5	20	5
Ppn6	2	0.5	0	30	5
Ppn7	3	0	0.5	30	5
Ppn8	3	0.25	0	40	5
Ppn9	3	0.5	0.25	20	5

The experimental setup used in the trials are presented in Figure 3.15. Each stage of the experiment is described in detail, item by item.

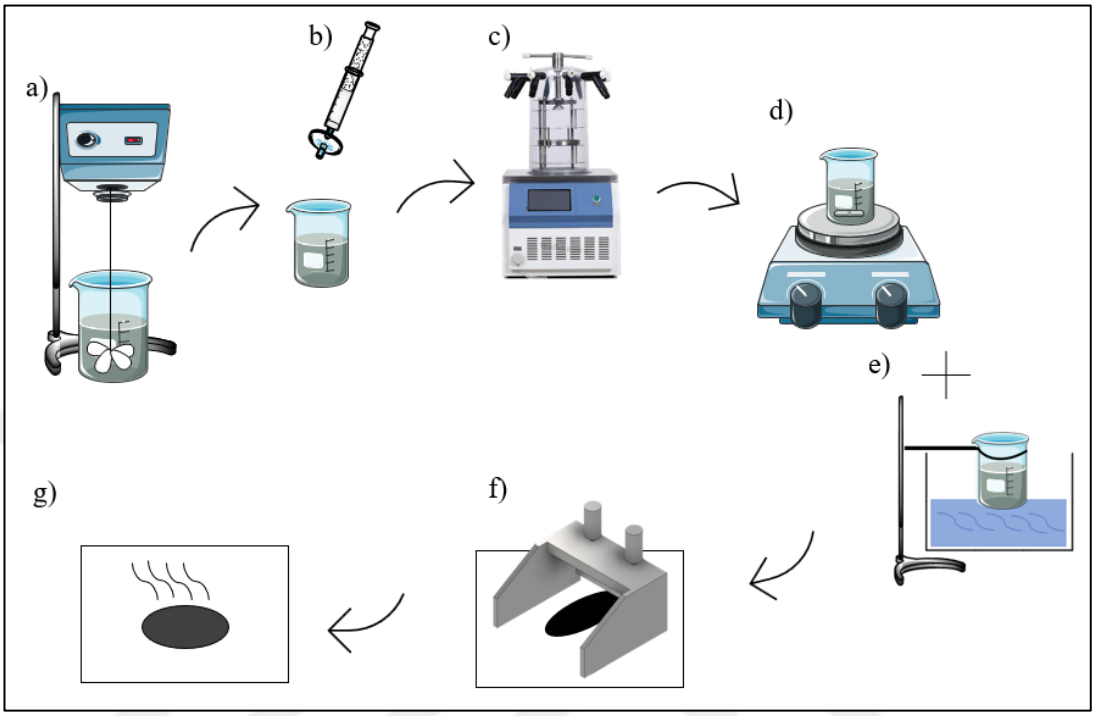

Figure 3.15 Experiment cycle

- The commercially purchased PEDOT: PSS was mixed in a mechanical mixer for 6 hours(a).
- It was passed through a 0.45 µm syringe filter (b).
- It was frozen with liquid nitrogen (b).
- It was lyophilized for 3 days (c).
- PEDOT: PSS was added to the DMSO-Water (15/85 v/v) mixture at the predetermined ratios (d).
- It was mixed in a magnetic stirrer for 5 minutes (d).
- Carbon-based materials were added to it at the predetermined ratios (d).
- It was mixed in a magnetic stirrer for 5 minutes (d).
- Lastly, Ag_2Se and sorbitol were added to it (d)
- It was mixed in an ultrasonic bath for 60 minutes followed by 30 minutes in a magnetic stirrer (in four cycles) (d-e)
- It was stirred in a magnetic stirrer for 72 hours (d)

- Films were made on the substrate using a blade (f)
- Films was left to dry under laboratory conditions for 48 hours (g)
- The dried films were removed from the substrate for characterization studies.

3.4 Characterization

Thermo Scientific Apreo S operating at 7.5-10 kV and the Carl Zeiss 300VP Scanning Electron Microscopy (SEM) operating at 15 kV were used to take SEM images.

EDX analysis was performed using the Carl Zeiss 300VP SEM instrument, and it was simultaneously analyzed while capturing the SEM images.

The electrical conductivity results were obtained using the four-probe technique. Measurement data obtained using the Keithley 2450 sourcemeter are presented in between Table 4.1 and Table 4.6 in the Results section.

Using the lab setup, the Seebeck coefficient of the created PEDOT: PSS-based mixtures was determined. Figure 3.16 shows the Seebeck coefficient measurement apparatus. The hot side of the material was heated within this framework using a thermoelectric module, and the cold side was kept at the ambient temperature. Next, the voltage variance across the surfaces was measured while current was applied between them. As a result, when the current flowing through the film was varied, the voltage between the two surfaces was observed, paying particular attention to the open-circuit (I=0) value at zero current. The scanning current range in the investigation was experimentally established at ±10 mA. The voltage levels were examined to ascertain the Seebeck coefficients at various temperatures once the current dropped to zero. N-type elements have a negative Seebeck coefficient, whereas P-type elements display a positive Seebeck coefficient, dependent on the direction of measurement.

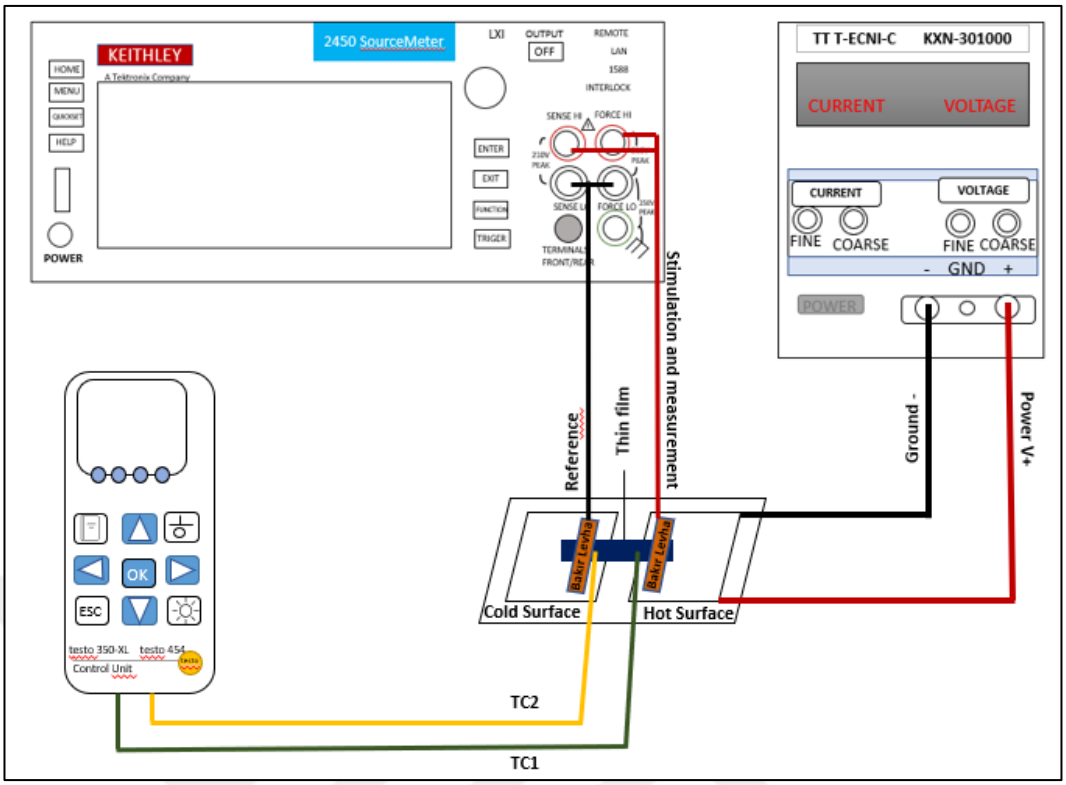

Figure 3.16 Seebeck Coefficient measurement setup

In thermoelectric materials, excellent power factor (Equation 3.1) is necessary for achieving high efficiency. Therefore, high-performance materials should possess high electrical conductivity and Seebeck coefficient.

$$PF = S^2\sigma \ [\mu W m^{-1} K^{-2}] \tag{3.1}$$

CHAPTER FOUR
RESULTS

SEM, Electrical Conductivity and Seebeck Coefficient results of this study are given below.

4.1 Scanning Electron Microscopy(SEM)

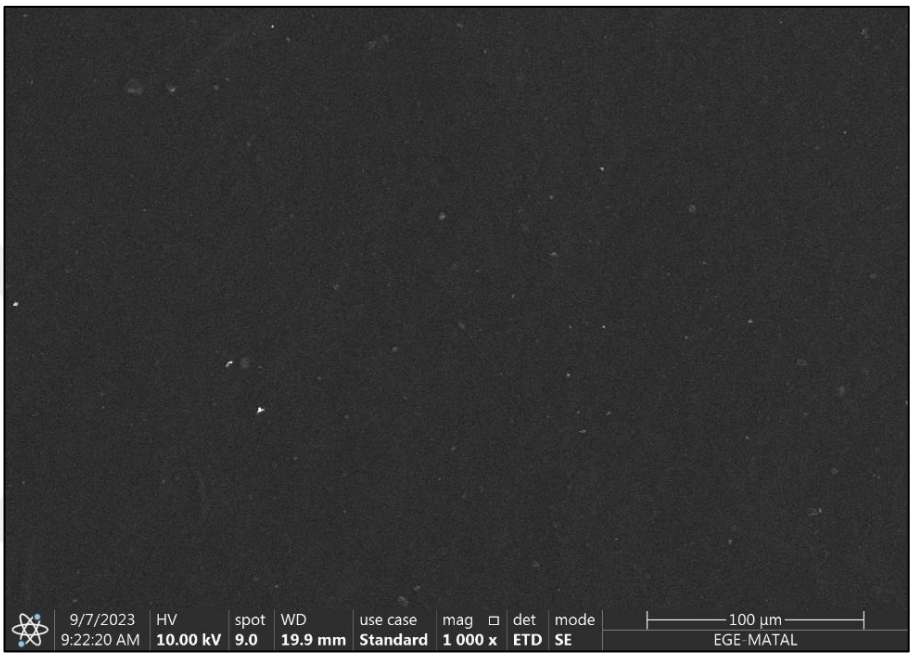

Figure 4.1 1% PEDOT: PSS Film

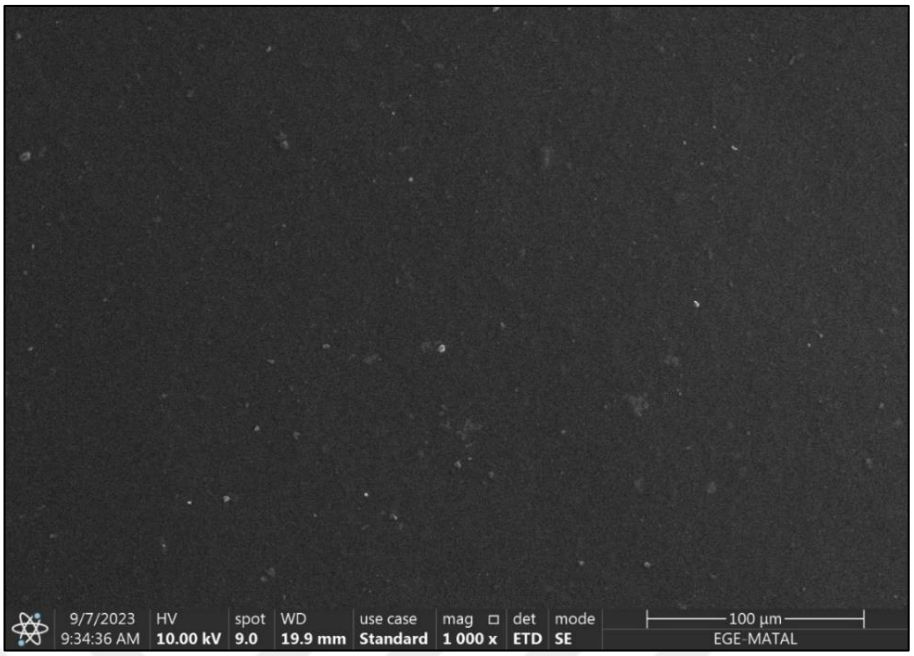

Figure 4.2 3% PEDOT: PSS film

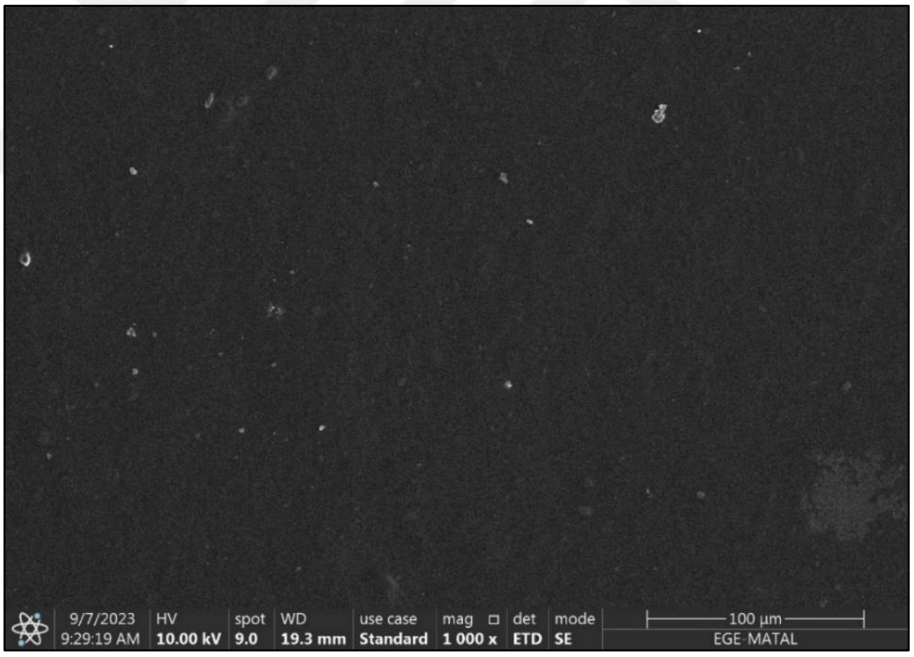

Figure 4.3 5% PEDOT: PSS Film

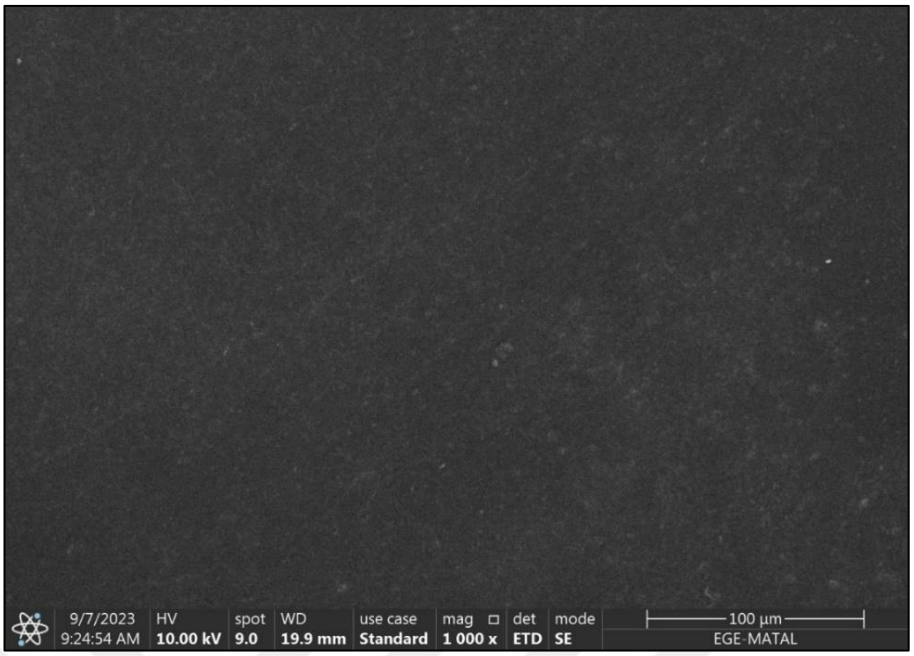

Figure 4.4 7% PEDOT: PSS Film

Between Figure 4.1- Figure 4.4, SEM images of films prepared with PEDOT: PSS are available. As seen in the figures, there are no signs of aggregation on the surface of the films.

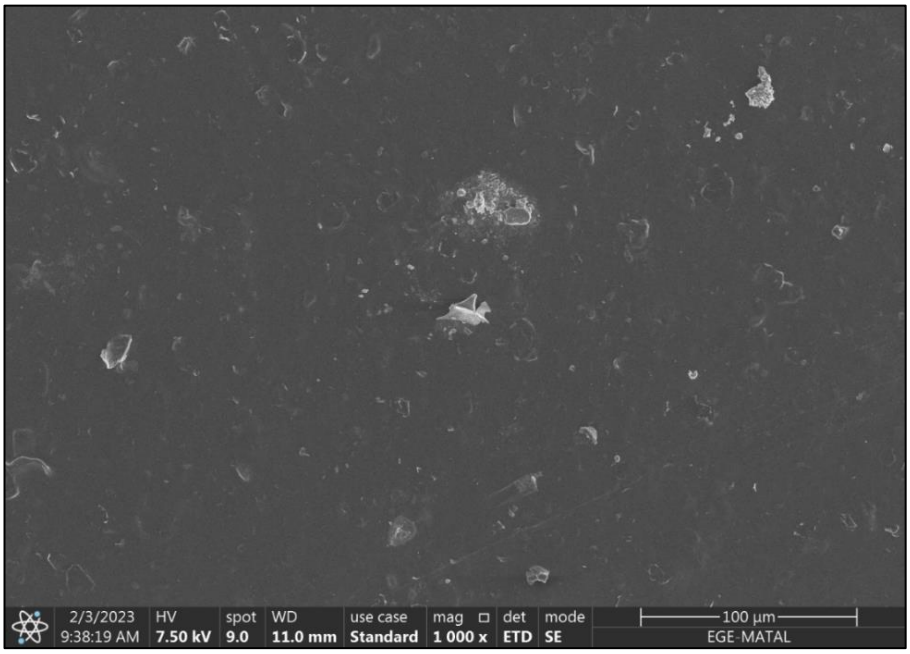

Figure 4.5 1% PEDOT: PSS+0,1% GR film

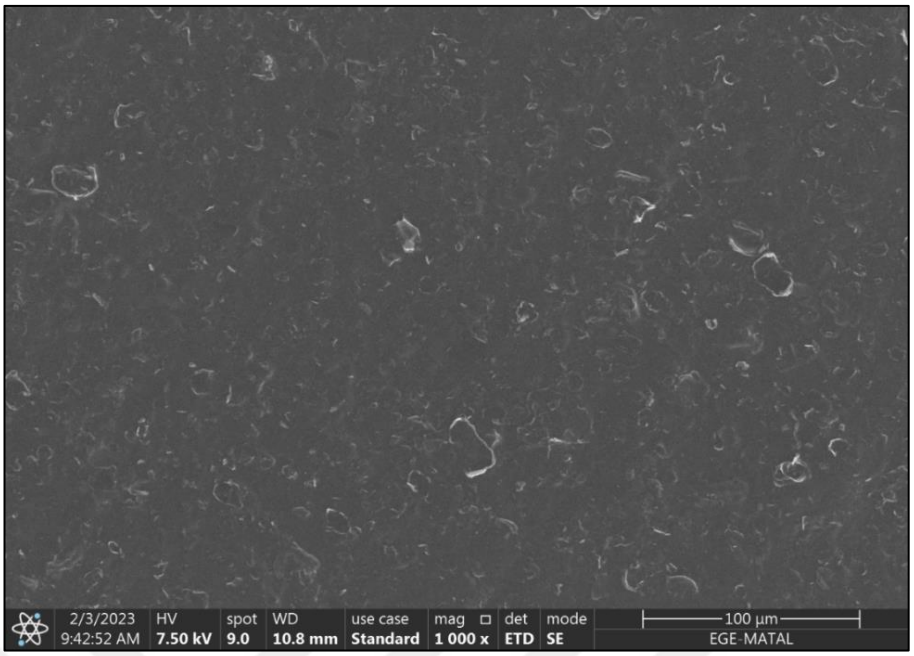

Figure 4.6 3% PEDOT: PSS+0,1% GR Film

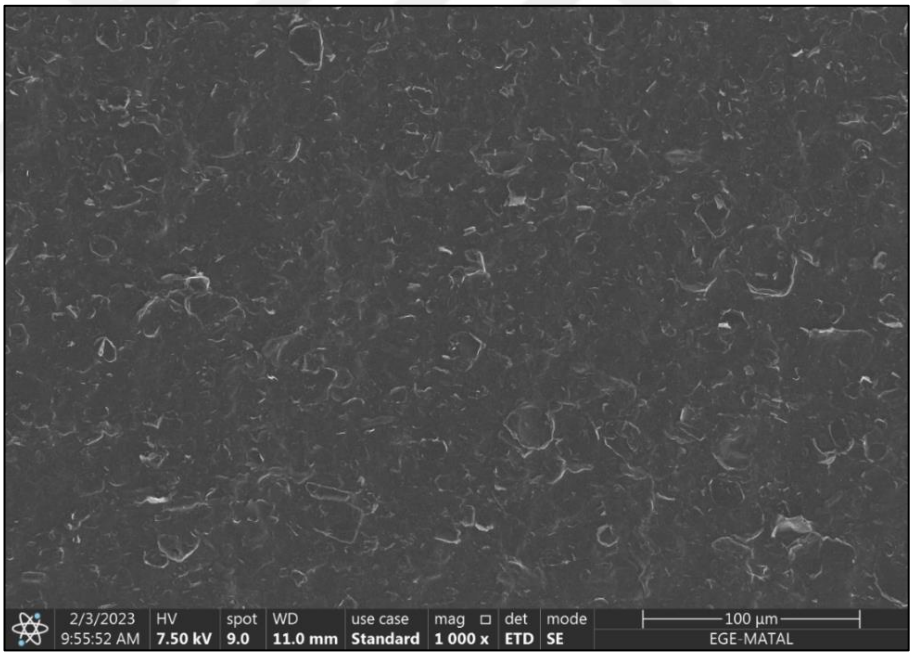

8

Figure 4.7 3% PEDOT: PSS+0,7% GR film

The images between Figure 4.5-Figure 4.7 depict films obtained from PEDOT: PSS/graphene mixtures. With an increase in the graphene ratio, an increase in the distribution of graphene within the film is observed. Graphene has a positive effect on

electrical conductivity, and its high conductivity properties positively impact the performance of such mixtures.

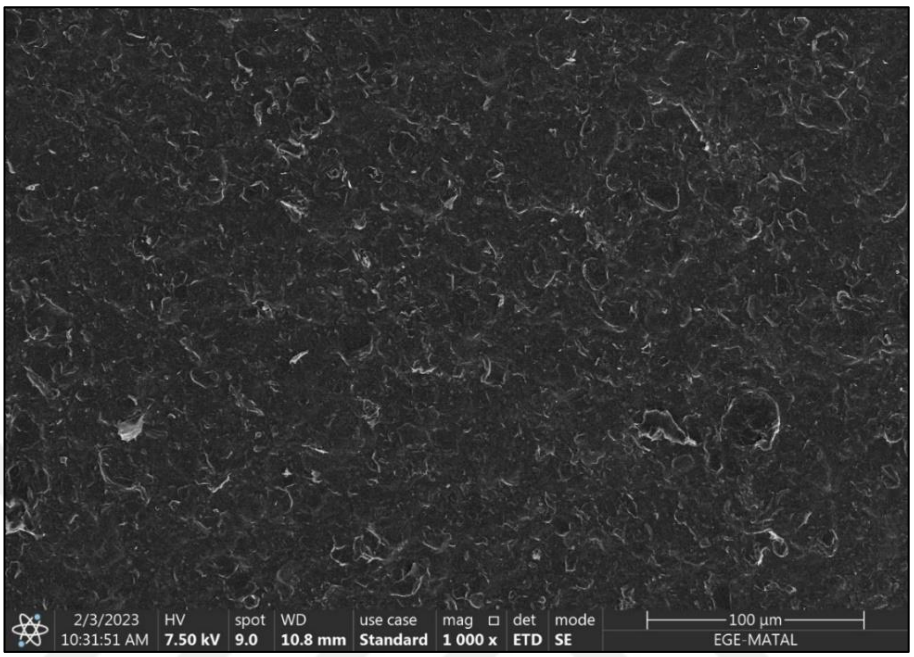

Figure 4.8 3% PEDOT: PSS+0,7% GR+0,1% CNTMW film

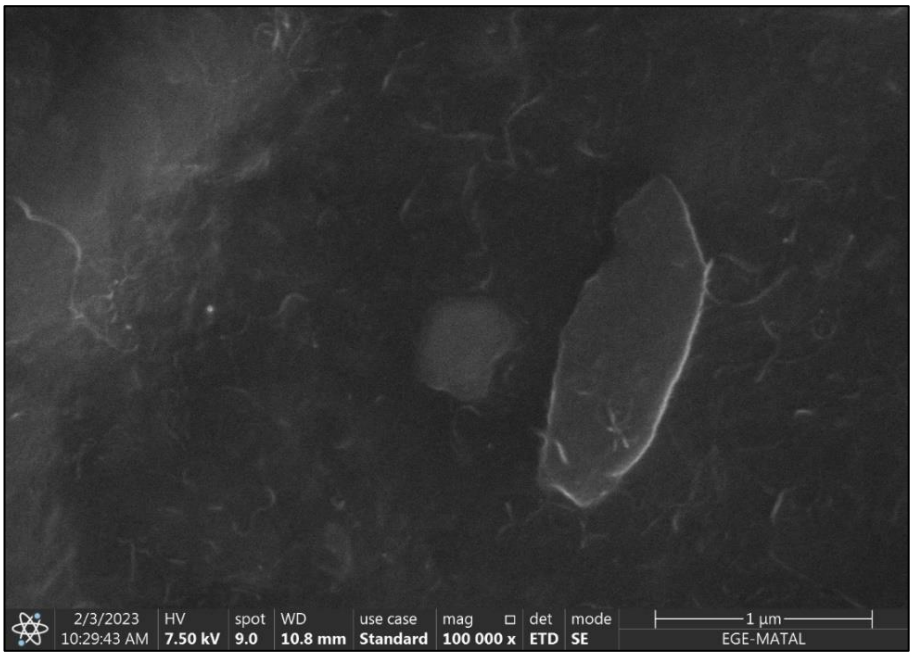

Figure 4.9 3% PEDOT: PSS+0,7% GR+0,1% CNTMW film-1

The images of a film prepared from a mixture containing 3% PEDOT: PSS, 0.7% graphene, and 0.1% CNTMW are available in Figure 4.8 and Figure 4.9, at different magnifications. In Figure 4.9, CNTMWs arranged around the graphene can be observed.

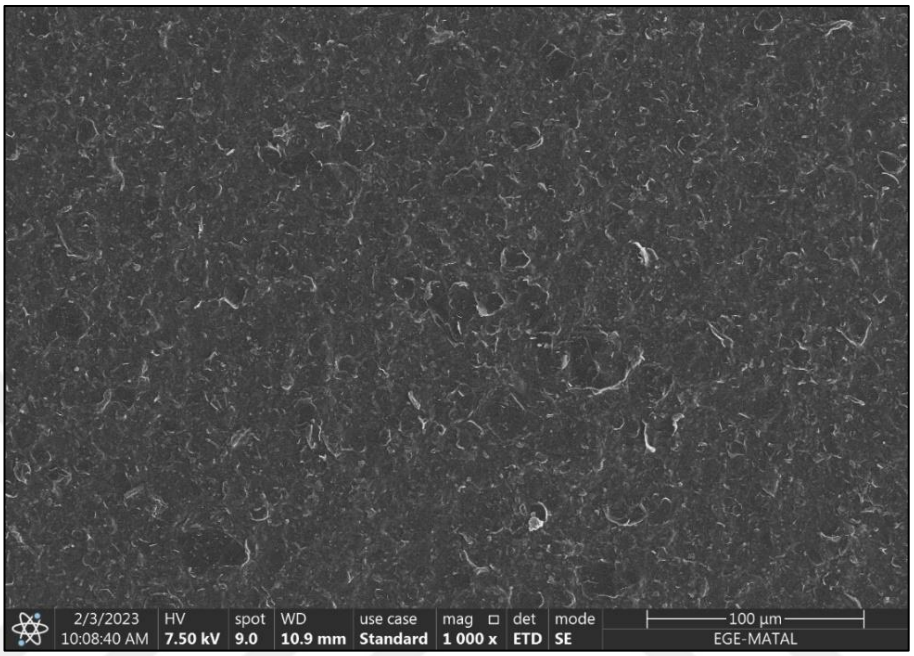

Figure 4.10 3% PEDOT: PSS+0,7% GR+0,7% CNTMW film

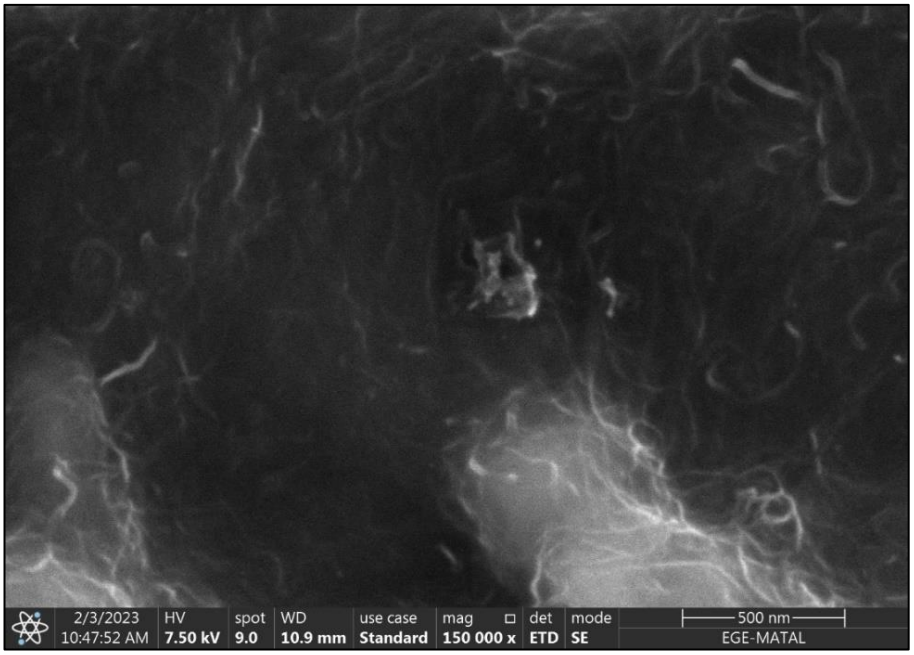

Figure 4.11 3% PEDOT: PSS+0,7% GR+0,7% CNTMW film-1

In Figure 4.10 and Figure 4.11, SEM images of a film prepared from a mixture containing 3% PEDOT:PSS, 0.7% graphene, and 0.7% CNTMW at different magnifications are available. As seen in the SEM image containing 0.7% CNTMW, CNTMWs are dispersed on the surface of the film, contributing to the increase in electrical conductivity.

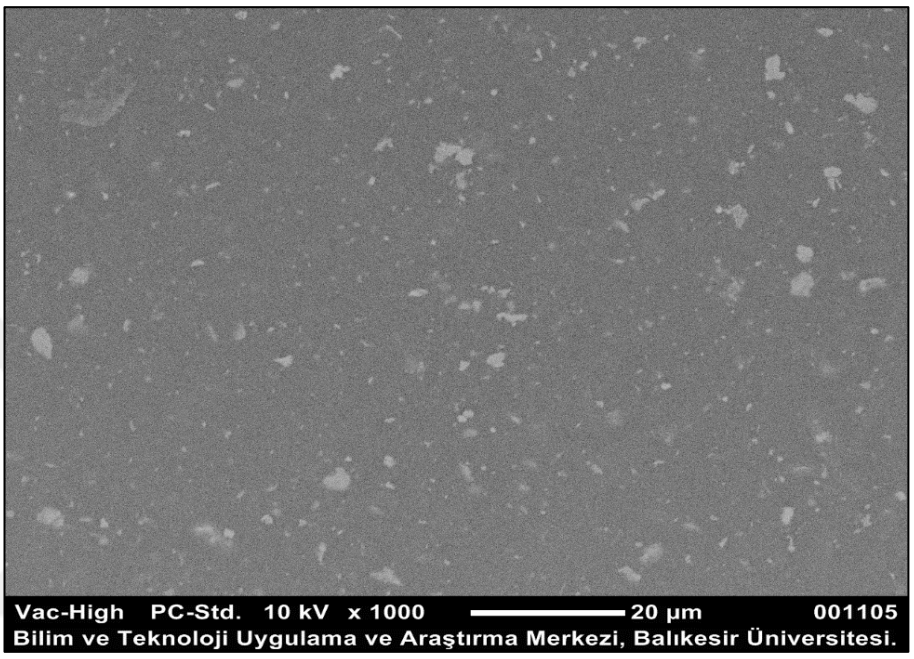

Figure 4.12 1% PEDOT: PSS/20% Ag_2Se film

In Figure 4.12, an SEM image of the film containing 1% PEDOT: PSS and 20% Ag2Se additive is provided. Within the film, it is observed that the Ag_2Se additive is unevenly distributed, and the particle sizes are not uniform. It is believed that this situation negatively impacts the measurements taken.

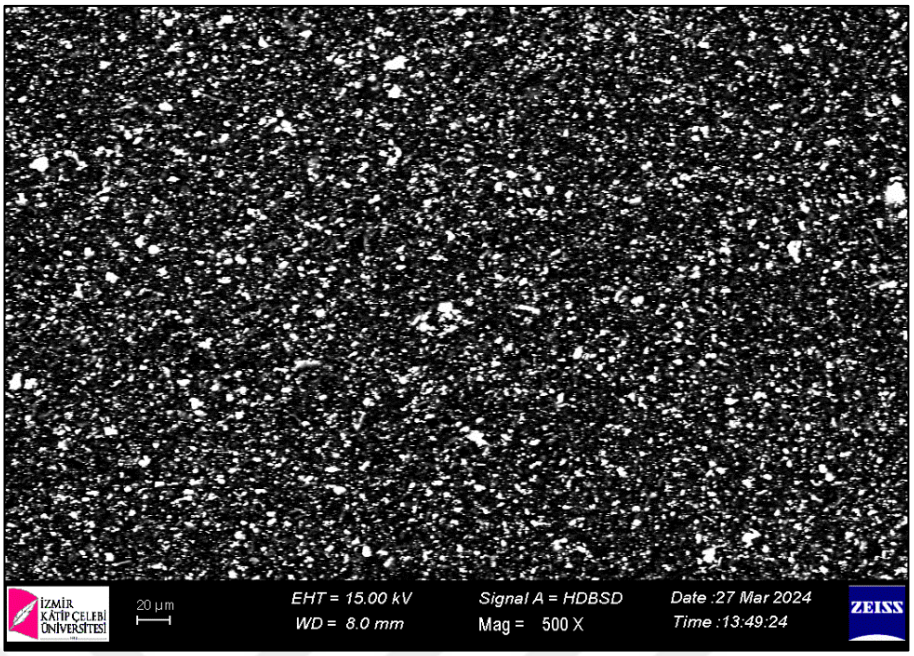

Figure 4.13 1% PEDOT: PSS/0.25% GR/0.25% CNTMW/30% Ag_2Se film

Figure 4.13 presents SEM images of the film containing carbon additive added to 1% PEDOT: PSS and Ag2Se additive. Due to the added carbon additives, it can be seen that Ag2Se is properly dispersed in the film and there is no agglomeration.

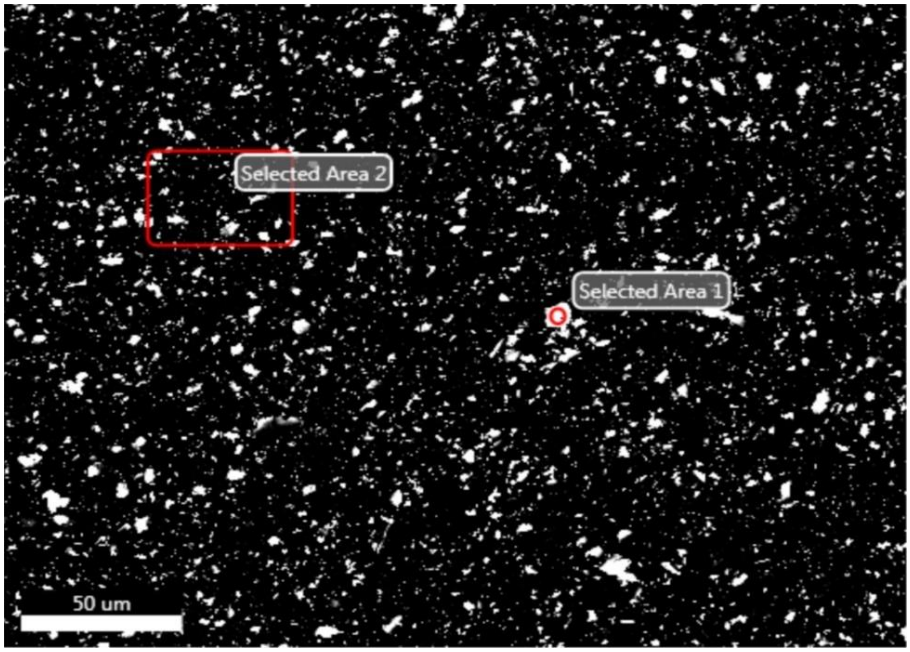

Figure 4.14 PPn2 SEM image with EDX analysis taken.

In Figure 4.14, an SEM image of the PPn2 mixture is presented. The results of the EDX analysis obtained from this are provided below.

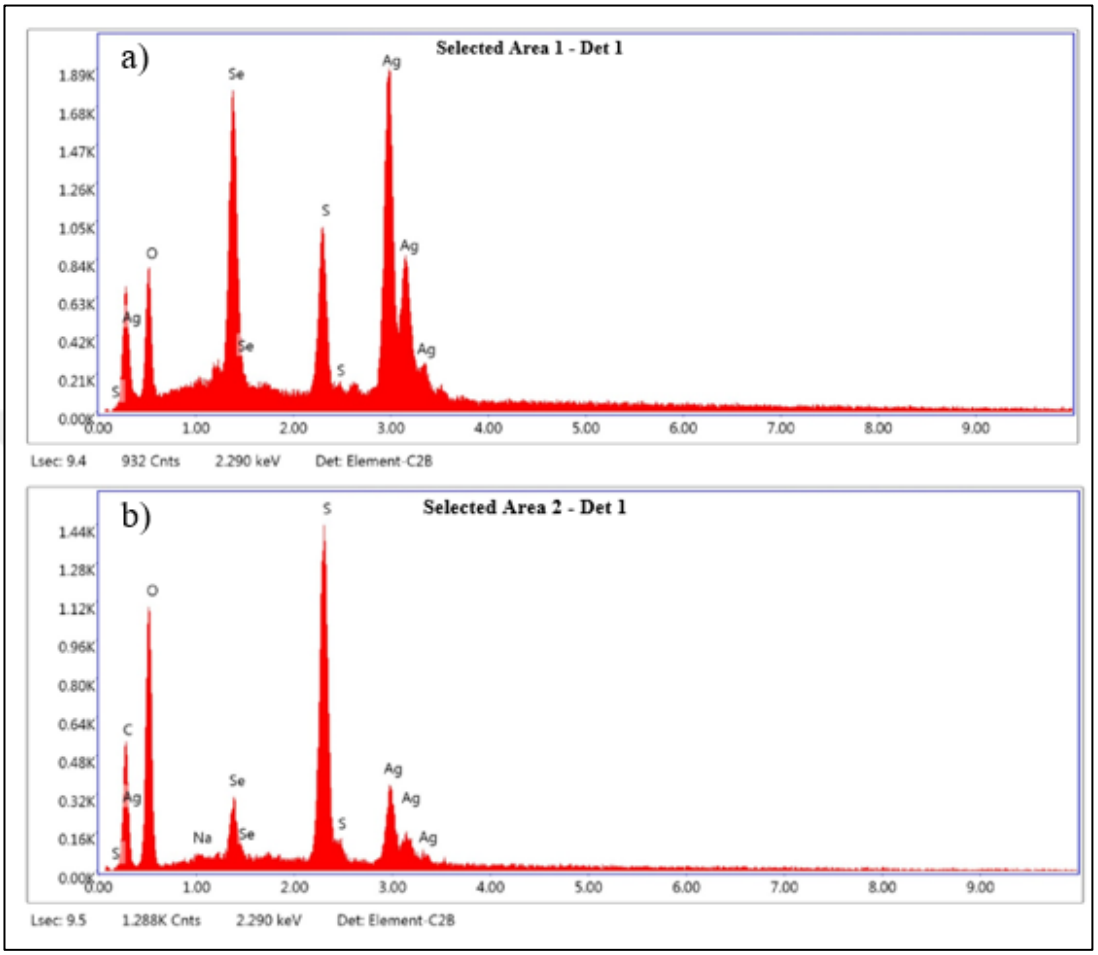

Figure 4.15 EDX analyses from PPn2 a) area 1 and b) area 2

Given the results of the EDX analysis(Figure 4.15) performed on Area 1 in Figure 4.14, it is predicated that the Ag_2Se structures are Ag_2Se-related due to the analysis's values. In addition, the analysis from Area 2, which covers a larger area, demonstrates that each component included in the composition of the material has been found.

4.2 Electrical Conductivity

Only a PEDOT: PSS film is displayed in Table 4.1, where the electrical conductivity values of films made with mixes of 1-3-5 and 7% PEDOT:PSS ratios are shown in Table 4.1. It has been noted that the electric conductivity of the produced film increases in correlation with the conductive polymer content in the mixture.

Table 4.1 Electrical conductivity of PEDOT: PSS in different concentrations

Material	**Electrical Conductivity(S/cm)**
PEDOT: PSS %1	3.10 ±0.07
PEDOT: PSS 3%	49.35±1.42
PEDOT: PSS 5%	97.28±0.6
PEDOT: PSS 7%	127.85±1.39

Table 4.1 presents the findings of an investigation into the electrical conductivities of carbon-doped materials that followed these experiments. Mixtures with 5% and 7% PEDOT: PSS in PEDOT: PSS/DMSO/Water solutions were found to have a high viscosity. It was discovered that the high viscosity of the combinations made it difficult to disperse the additives within them and produce films from them. Consequently, mixtures containing 5% and 7% PEDOT: PSS were not used in the studies that followed.

The obtained materials' electrical conductivity is shown in Table 4.2. It is found that the ratios of polymer, graphene, and CNTMW in the film are directly correlated with the electrical conductivity.

Table 4.2 Electrical conductivity in different ratios of PEDOT:PSS/GR/CNTMW

Materials	Electrical Conductivity (S/cm)
PEDOT: PSS 1%	3.10 ±0.07
PEDOT: PSS 3%	111.93 ±3.63
PEDOT: PSS 3% + 0.1% GR	119.3 ±0.77
PEDOT: PSS 3% + 0.3% GR	139.9 ±0.98
PEDOT: PSS 3% + 0.5% GR	157.57 ±2.98
PEDOT: PSS 3% + 0.7% GR	162.62 ±0.70
PEDOT: PSS 3% + 0.7% GR+0.1% CNTMW	173.08 ±0.72
PEDOT: PSS 3% + 0.7% GR+0.3% CNTMW	176.01 ±1.04
PEDOT: PSS 3% + 0.7% GR+0.5% CNTMW	187.42 ±2.17
PEDOT: PSS 3% + 0.7% GR+0.7% CNTMW	190.17 ±0.67

The effects of PEDOT: PSS, graphene, and CNTMW content within the film on the electrical conductivity were investigated. Based on the obtained data, the experimental design for P and N-type materials was determined using the Taguchi method.

The electrical conductivities of films made from P-type materials are available in Table 4.3. As illustrated in the table, the material with the highest electrical conductivity belongs to PPp9 (3% PEDOT: PSS, 0.50% graphene, and 0.25% CNTMW).

Table 4.3 P- type materials electrical conductivity values

Material of p-type	Electrical Conductivity (S/cm)
PPp1	19.73±0.59
PPp2	22.89±0.42
PPp3	26.80±0.34
PPp4	46.30±0.76
PPp5	41.60±0.91
PPp6	43.21±0.74
PPp7	61.38±0.83
PPp8	80.96±0.72
PPp9	86.90±0.76

The Table 4.4 includes the electrical conductivities of films identified as N-type. As observed in the table, material PPn7 (3% PEDOT: PSS, 0.5% CNTMW, and 30% Ag_2Se) exhibits the highest electrical conductivity.

Table 4.4 N- type materials electrical conductivity values

Material of n-type	Electrical Conductivity (S/cm)
PPn1	30.77±0.61
PPn2	26.55±0.70
PPn3	35.87±0.20
PPn4	45.17±0.60
PPn5	49.02±0.63
PPn6	52.90±0.77
PPn7	67.42±0.64
PPn8	65.92±0.67
PPn9	60.97±0.52

Figure 4.16 Electrical conductivity results using the Taguchi method presents the electrical conductivity results of films prepared with Pedot PSS-based mixtures based

on the Taguchi method. As evident in both graphs, a rise in the ratios of PEDOT: PSS, and graphene correlates with a boost in electrical conductivity. The graph for P-type materials is depicted in Figure 4.16 a, indicating fluctuating effects of CNTMW and Ag_2Se additives on electrical conductivity and displaying contrasting characteristics. The graph for N-type materials is shown in Figure 4.16 b, revealing that an elevation in the ratios of Ag_2Se, PEDOT: PSS, and graphene within the film leads to a growth in electrical conductivity.

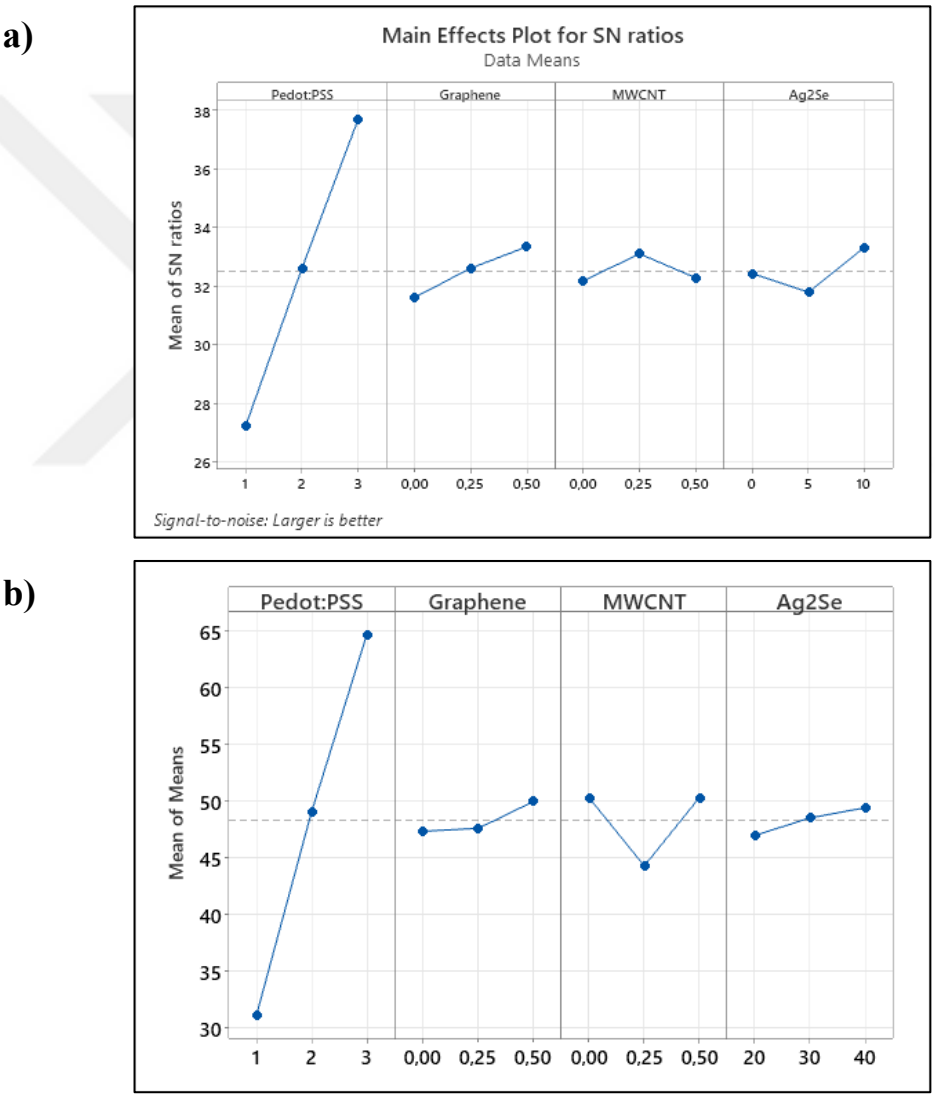

Figure 4.16 Electrical conductivity results using the Taguchi method a) P-Type Material b) N-Type Material

4.3 Seebeck Coefficient

The Seebeck coefficients of films prepared with mixtures containing 1%, 3%, 5%, and 7% PEDOT: PSS were measured, and the results are presented in Figure 4.17. While an increase in the proportion of conductive polymer from 1% to 5% resulted in an increase in the Seebeck coefficient, the film obtained from the mixture containing 7% PEDOT: PSS exhibited a lower Seebeck coefficient than expected. This discrepancy, as also explained in the electrical conductivity section, arises from the hindrance of ideal film formation due to high viscosity.

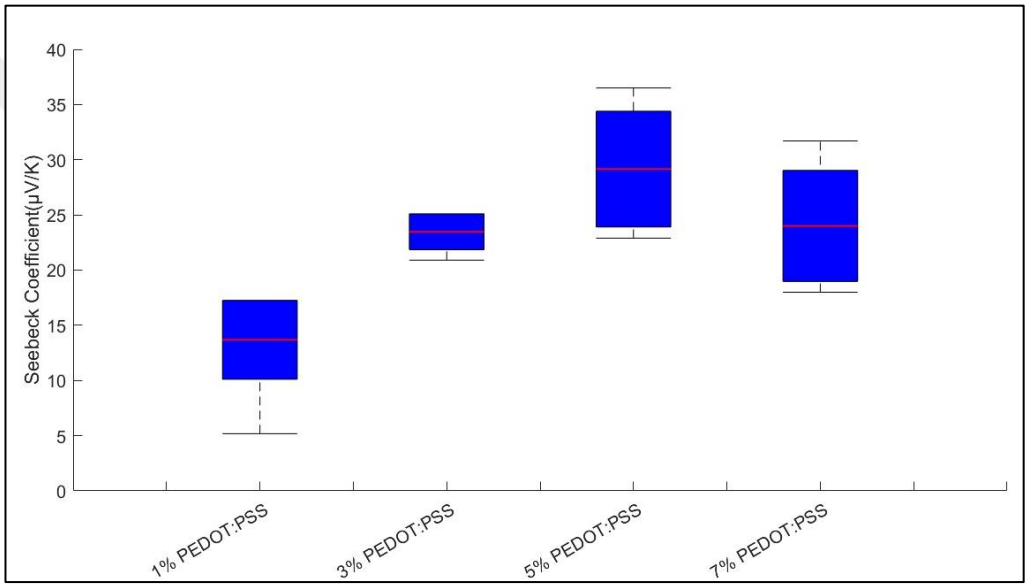

Figure 4.17 Seebeck Coefficient results for PEDOT: PSS

When not containing any additives, the PEDOT: PSS polymer, exhibiting behaviors characteristic of P-type materials, indeed yielded positive Seebeck coefficients as expected.

The results of the investigation into the impact of graphene and CNTMW on the Seebeck coefficient of PEDOT: PSS are shown in Figure 4.18. It is observed that the Seebeck coefficient is found to rise when 0.1% and 0.3% graphene are added to the film matrix; however, bigger amounts of additional graphene have the opposite effect. Moreover, it is noted that the Seebeck coefficient decreases upon the addition of CNTMW to the film matrix following to the inclusion of graphene.

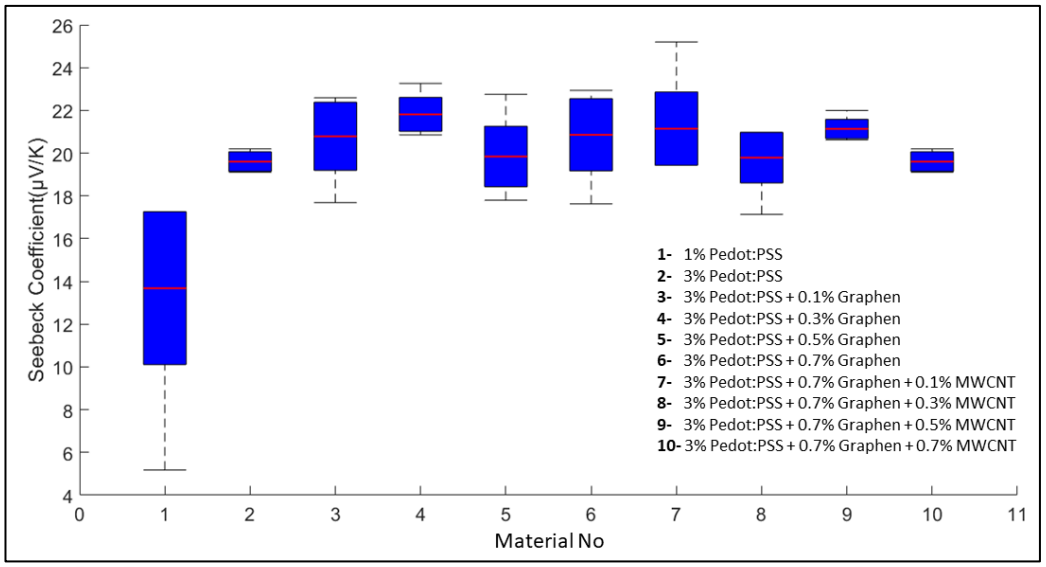

Figure 4.18 Seebeck coefficient results for PEDOT: PSS/GR/CNTMW films

To convert the P-type characteristics of the PEDOT: PSS polymer into N-type, the electron carrier Ag_2Se has been incorporated into the film matrix. The Seebeck coefficients of the PEDOT: PSS films, which have been transformed into N-type by the addition of Ag_2Se, are presented in Figure 4.19.

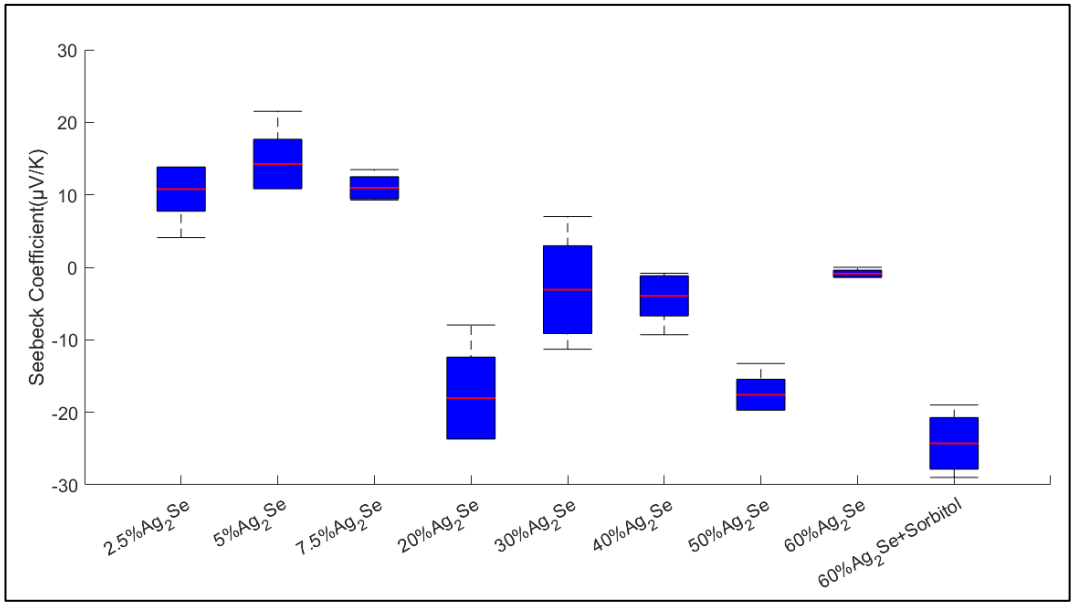

Figure 4.19 Seebeck coefficient results for PEDOT: PSS/Ag_2Se films

As seen in Figure 4.19, when Ag_2Se is added in proportions of less than 20%, the characteristic properties of the PEDOT: PSS polymer dominate, and the film behaves like a P-type material. However, when the proportion of Ag_2Se exceeds 20%, the film exhibits behavior akin to N-type. Despite the expectation of a negative escalate in the Seebeck coefficient with an escalate in the proportion of Ag_2Se within the material, this phenomenon was not observed at proportions of 30%, 40%, and 60%. These films containing high amounts of Ag_2Se, the heterogeneous accumulation of Ag_2Se at the base of the film during drying caused the film to behave like two different materials layered on top of each other rather than a single material, resulting in irregularities in the Seebeck coefficients. To prevent the heterogeneous accumulation of Ag_2Se within the film, sorbitol was added to the film as a plasticizer and dispersant. It was found that the Seebeck coefficient of the film containing 60% Ag_2Se exhibited the highest negative value, stabilized by sorbitol, which distributed the excess Ag_2Se particles within the film.

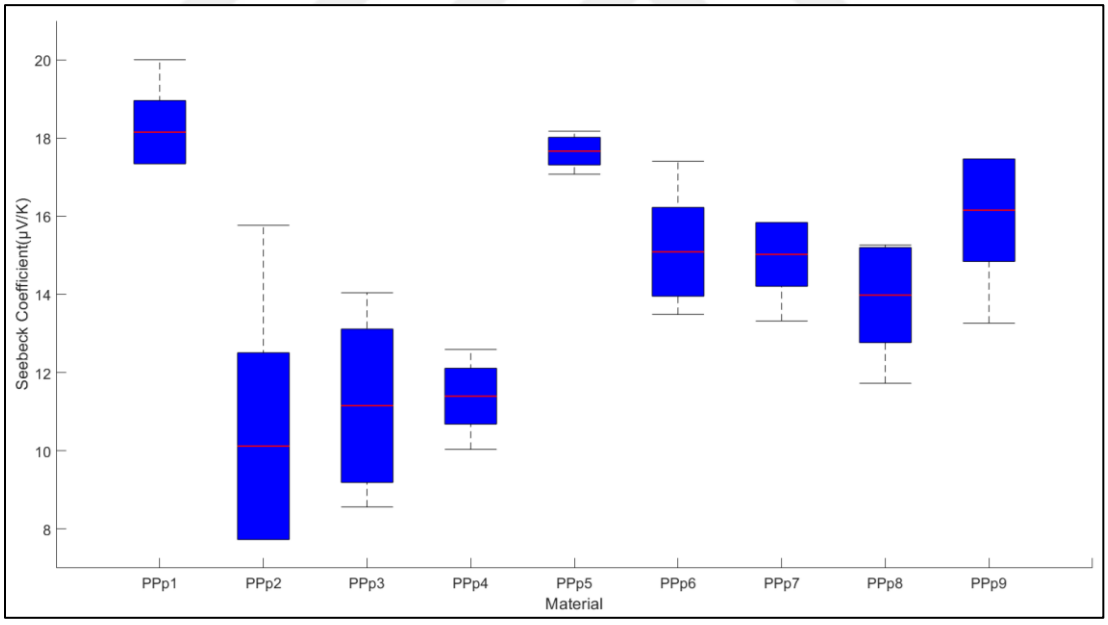

Figure 4.20 Seebeck Coefficient results for p-type materials

The Seebeck coefficients of films prepared using the Taguchi method were measured and are presented in Figure 4.20. The film with the highest Seebeck coefficient was obtained from the mixture was coded as PPp1. This mixture contains 1% PEDOT: PSS and 5% sorbitol. When compared to the film obtained from the

mixture containing 1% PEDOT: PSS, it is observed that the film containing 5% sorbitol has a higher Seebeck coefficient.

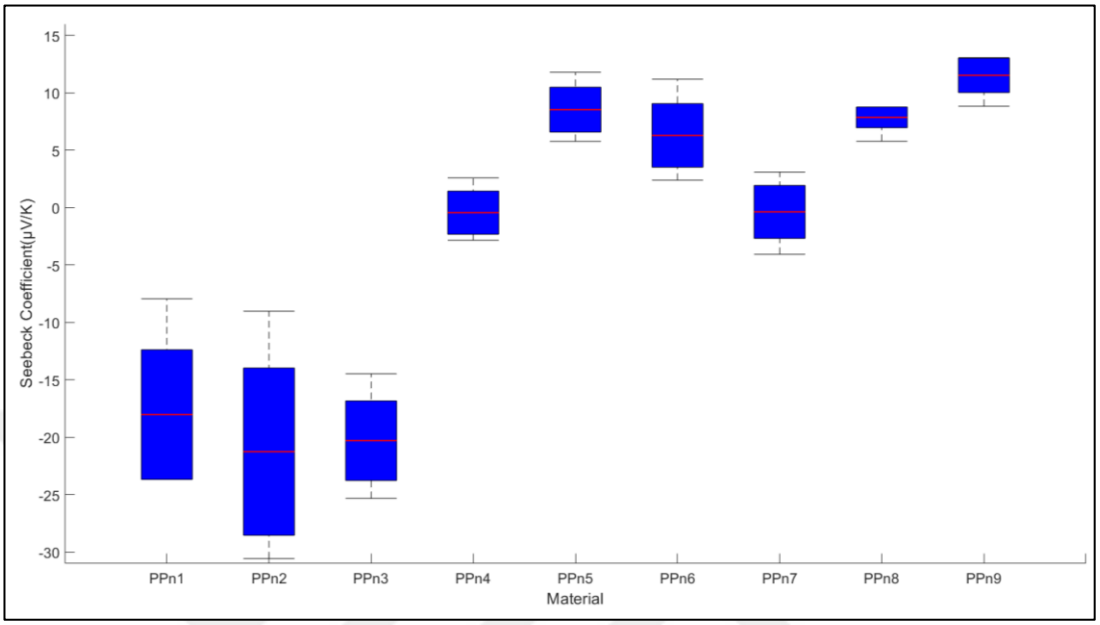

Figure 4.21 Seebeck Coefficient results for N-type Materials

Figure 4.21 provides the measurement results of the Seebeck coefficient for films designed as N-type materials. PEDOT: PSS and carbon-based additives impart P-type characteristics to the film, whereas the high proportion of added Ag_2Se confers N-type properties. The proportion of Ag_2Se has only shown the necessary effect in films coded as PPn1-2-3, enabling the transformation of materials from P-type to N-type.

Measurements were taken with temperature differences (ΔT) of 5-20-35°C between the surfaces of the films. While Figure 4.22 depict the Seebeck coefficient results for P-type materials, Figure 4.23 show the Seebeck coefficient for N-type materials.

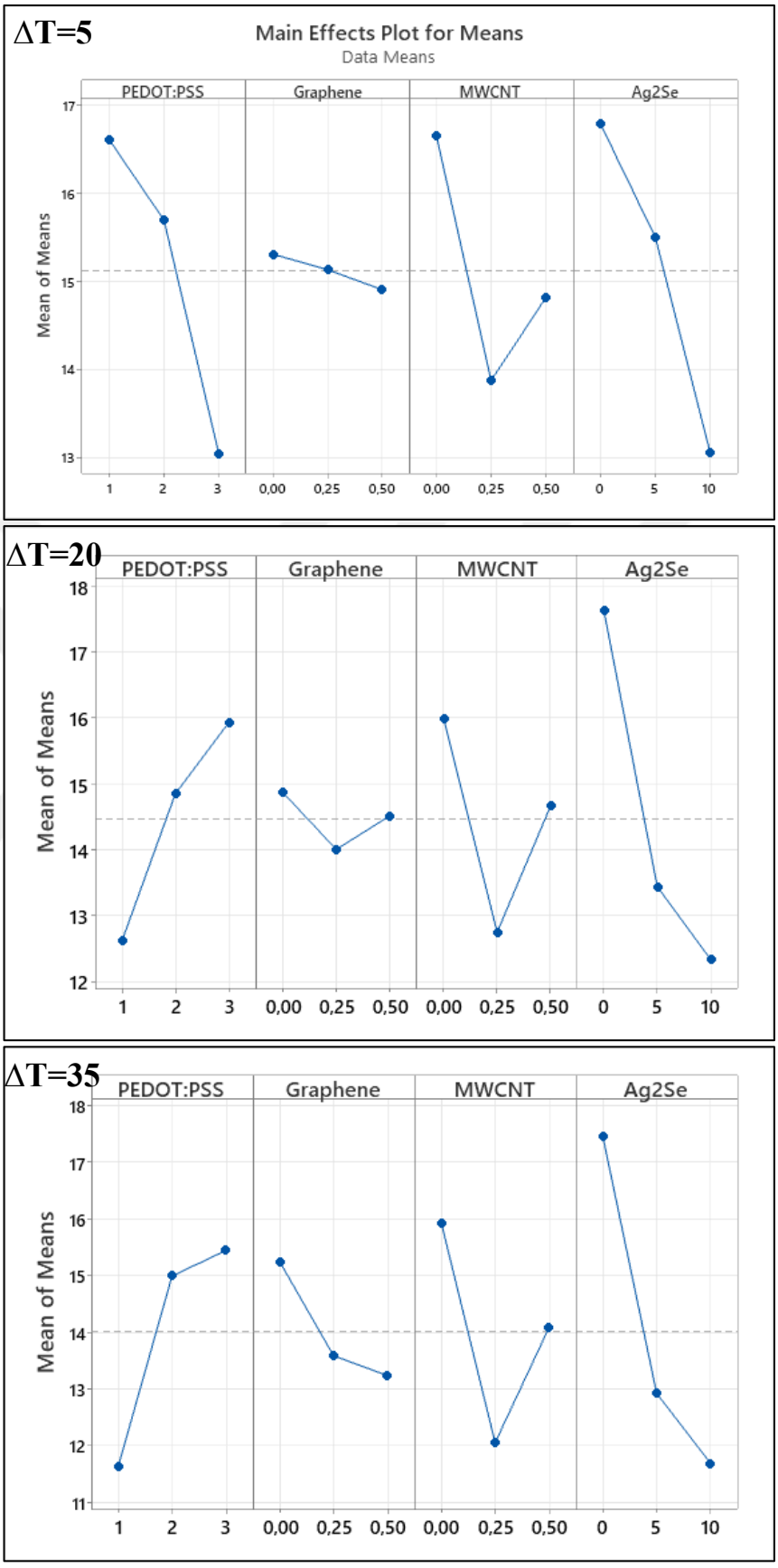

Figure 4.22 Seebeck coefficient results using the Taguchi method (P-Type Material)

P-Type Materials;

The Seebeck coefficient of the material incorporating 3% PEDOT: PSS is notably higher when the temperature differences are 20 and 35 compared to those containing 1% and 2%. However, at a temperature difference of 5, the film with 1% PEDOT: PSS exhibits a higher Seebeck coefficient than those with 2% and 3% PEDOT: PSS. When Ag_2Se was introduced into the material, there is a decline in the Seebeck coefficient as the material's behavior shifts from P-type to N-type. Specifically for P-type materials, the lowest Seebeck coefficients were observed, with the film containing 10% Ag_2Se identified as having the lowest Seebeck coefficient. Carbon-based materials demonstrate consistent effects on the Seebeck coefficient across various temperature differences.

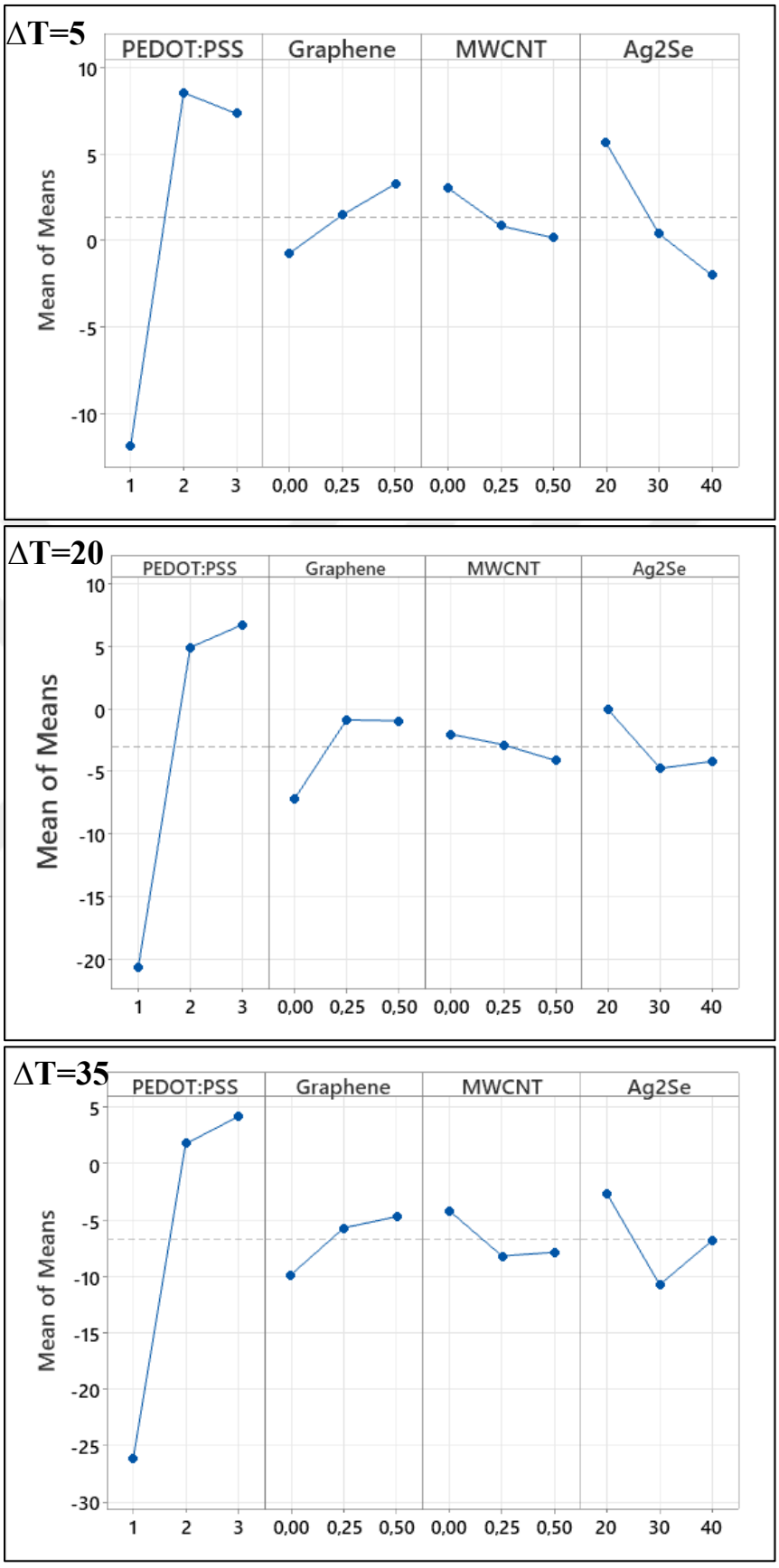

Figure 4.23 Seebeck coefficient results using the Taguchi method (N-Type Material)

N-Type Materials;

The parameter that most significantly influences the Seebeck coefficient is the ratio of PEDOT:PSS within the film, with the material containing 1% PEDOT: PSS being ideal for the preparation of N-type films. As the proportion of Ag_2Se within the film increases, the N-type characteristic of the film intensifies. When the temperature difference is 5, the optimal ratio is determined to be 40%, while for temperature differences of 20 and 35, the optimal ratio is determined to be 30% Ag_2Se.

Table 4.5 P- type materials electrical conductivity and thermoelectric properties

	Electrical Conductivity (S/cm)	**Seebeck Coefficient(μV/K)**	**Power Factor (μW/mK²)**
PPp1	19.73±0.59	18.20	0.65
PPp2	22.89±0.42	8.12	0.15
PPp3	26.80±0.34	8.56	0.20
PPp4	46.30±0.76	11.91	0.66
PPp5	41.60±0.91	18.05	1.36
PPp6	43.21±0.74	15.02	0.97
PPp7	61.38±0.83	15.62	1.50
PPp8	80.96±0.72	14.58	1.72
PPp9	**86.90±0.76**	**16.12**	**2.26**

Table 4.6 N- type materials electrical conductivity and thermoelectric properties

	Electrical Conductivity (S/cm)	**Seebeck Coefficient (μV/K)**	**Power Factor ($\mu W/mK^2$)**
PPn1	30.77±0.61	-22.69	1.58
PPn2	**26.55±0.70**	**-30.57**	**2.48**
PPn3	35.87±0.2	-25.33	2.30
PPn4	45.17±0.60	-2.85	0.04
PPn5	49.02±0.63	5.77	0.16
PPn6	52.90±0.77	2.39	0.03
PPn7	67.42±0.64	-4.07	0.11
PPn8	65.92±0.67	7.67	0.39
PPn9	60.97±0.52	8.82	0.47

The calculated power factor (PF) values for P-type materials are provided in Table *4.5*, while those for N-type materials are presented in Table 4.6. For a thermoelectric material to exhibit high performance, it is imperative to possess a high PF. As evident from the tables, sample PPp9, designed for P-type materials, and sample PPn2, designed for N-type materials, yield the highest PF values.

CHEPTER FIVE
CONCLUSIONS

The data obtained throughout the study was examined and the observations and results of the study are given below.

• Bases with an adequate level of hydrophilicity are desirable for facilitating the uniform spreading of the film and its subsequent easy release from the surface upon drying. Furthermore, bases demonstrating both flexibility and hydrophobic properties are preferred to ensure the film's facile removal. In the context of coating-style film production, the utilization of hydrophilic bases enables effective surface coating procedures.

• It has been observed that as the drying temperature increases, films become more fragile and adhere tightly to all surfaces regardless of their physical properties, remaining attached without deformation.

• As the PEDOT:PSS ratio in the film increases, electrical conductivity increases.

• As the concentrations of MCWNT and graphene in the film increase, the electrical conductivity of the film increases, but when the two materials are added into the film at the same time, sometimes a reduce in electrical conductivity and sometimes less than expected increases are observed. When the data are examined, it is thought that these two carbon-based materials may have a negative effect on each other. In addition, since the concentrations of carbon-based materials are relatively low, this negative effect can be seen. Their effects can be observed more clearly at higher ratios.

• The Seebeck coefficient stands as one of the most crucial effects for thermoelectric materials. The Seebeck coefficient increases more positively with increasing PEDOT:PSS ratio. While this is a desired feature for P-type films, it is an undesirable feature for N-type materials. Although carbon-based materials do not have a dominant effect on Seebeck, it is thought that their effect may become more dominant at larger amounts. As the concentration of Ag_2Se, a semiconductor material added to the solution, increases, the Seebeck coefficient decreases. This is a negative effect in P-type materials, and a positive effect in N-type materials.

• The power factor term is obtained by its linear effect with electrical conductivity and its second-order effect with the Seebeck coefficient. Therefore, films with high

electrical conductivity and high Seebeck coefficient should be preferred. In this context, studies carried out to increase these two values are studies that increase thermoelectric performance.

In the study, promising results were obtained on electrical conductivity and Seebeck coefficient. In future studies, the chemical interactions of the additives added to the film and the mechanisms by which these interactions affect the Seebeck coefficient and electrical conductivity should be clarified.

REFERENCE

Alshabouna, F., Lee., H. S., Barandun, G., Tan, E., Çotur, Y., Asfour, T., Gonzalez-Macia L., Coatsworth, P., Núnez-Bajo, E., Kim, J., & Güder, F., 2022. "PEDOT:PSS-Modified Cotton Conductive Thread for Mass Manufacturing of Textile-Based Electrical Wearable Sensors by Computerized Embroidery". *Materials Today* 59:56-67. doi: 10.1016/j.mattod.2022.07.015.

Aydin, Y. (2012). İletken Polimerlerin İçerisinde Enzim Tutuklanmasıyla Yapılan Biyosensörler. [Unpublished doctoral dissertation] Karamanoğlu Mehmetbey University.

Bednarczyk, K., Matysiak, W., Tański, T., Janeczek, H., Schab-Balcerzak, E., & Libera M., 2021. Effect of Polyaniline Content and Protonating Dopants on Electroconductive Composites. *Scientific Reports* 11(1):7487. doi: 10.1038/s41598-021-86950-4.

Benchirouf, A., Palaniyappan, S., Ramalingame, R., Raghunandan, P., Jagemann, T., Müller, C., Hietschold, M., & Kanoun, O., 2016. Electrical Properties of Multi-Walled Carbon Nanotubes/PEDOT:PSS Nanocomposites Thin Films under Temperature and Humidity Effects. *Sensors and Actuators B: Chemical* 224:344-50. doi: 10.1016/j.snb.2015.10.009.

Boeva, Zh. A., & V. G. Sergeyev. 2014. Polyaniline: Synthesis, Properties, and Application. *Polymer Science Series C* 56(1):144-53. doi: 10.1134/S1811238214010032.

Crispin, X., Marciniak, S., Osikowicz, W., Zotti, G., Van Der Gon, A. D., Louwet, F., & Salaneck, W. R. (2003). Conductivity, morphology, interfacial chemistry, and stability of poly (3, 4-ethylene dioxythiophene)–poly (styrene sulfonate): A photoelectron spectroscopy study. Journal of polymer science Part B: Polymer physics, 41(21), 2561-2583. doi: 10.1002/polb.10659.

Derebaşı, N. (2015). Termoelektrik Soğutma Hücrelerinde Geometrik Yapısal Etkilerin İncelenmesi. [Unpublished doctoral dissertation] Bursa Uludağ University.

Feldman, D. (2008). Polymer history. Designed monomers and polymers, 11(1), 1-15. doi: 10.1163/156855508X292383.

Feng, K., Xu, L., Xiong, Y., Sun, L., Yu, H., Wu, M., Thant, A. A., & Hu, B. (2020). PEDOT: PSS and Ni-Based Thermoelectric Generator for Solar Thermal Energy Conversion. *Journal of Materials Chemistry C* 8(11):3914-22. doi: 10.1039/C9TC06277G.

Gaurav, K., SanthiBhushan, B., Mino-Galaz, G., Gutierrez, G., & Srivastava, A. (2021). Hybridization and Torsion Defects Influenced Electron Transport in Trans-Polyacetylene. *Physica E: Low-Dimensional Systems and Nanostructures* 129:114628. doi: 10.1016/j.physe.2021.114628.

Green, R., & Abidian M. R. (2015). Conducting Polymers for Neural Prosthetic and Neural Interface Applications. *Advanced Materials* 27(46):7620-37. doi: 10.1002/adma.201501810.

Güldiken, F. (2011). Termoelektrik Modüllerin Fiziksel Boyutlarının Soğutma Kapasitesi Üzerine Etkisinin Sonlu Elemanlar Yöntemi ile Modellenmesi. [Unpublished master dissertation] Bursa Uludağ University.

Han, M., Erdost Y., Kaleli, H. N., Karaz S., Eren G. O., Dogru-Yuksel, I. B., Senses, E., Şahin, A., & Nizamoglu S. (2022). Tissue-Like Optoelectronic Neural Interface Enabled by PEDOT:PSS Hydrogel for Cardiac and Neural Stimulation. *Advanced Healthcare Materials* 11(8):2102160. doi: 10.1002/adhm.202102160.

He, H. & Ouyang, J. (2020). Enhancements in the Mechanical Stretchability and Thermoelectric Properties of PEDOT:PSS for Flexible Electronics Applications. *Accounts of Materials Research* 1(2):146-57. doi: 10.1021/accountsmr.0c00021.

Horii, T., Hikawa, H., Katsunuma, M., & Okuzaki, H., (2018). Synthesis of Highly Conductive PEDOT:PSS and Correlation with Hierarchical Structure. *Polymer* 140:33-38. doi: 10.1016/j.polymer.2018.02.034.

Huang, M., Lee, S., Jo, I. Y., Park, H., Shim, B. S., & Yoon, M. H. (2024). One-step wet-spinning of conducting polymer and cellulose nanofiber composites for fiber-type organic electrochemical transistors. Carbohydrate Polymers, 324, 121559. doi: 10.1016/j.carbpol.2023.121559.

Hudson, Bruce. (2018). Polyacetylene: Myth and Reality. *Materials* 11(2):242. doi: 10.3390/ma11020242.

Husain, A., Ahmad, S., Alqarni, S. A., Almehmadi, S. J., Yatoo, M. A., Habib, F., & Shariq, M. U. (2023). Conductive polythiophene/graphitic-carbon nitride nanocomposite for the detection of ethanol mixing in petrol. RSC advances, 13(18), 12080-12091. doi: 10.1039/D3RA00381G

Hüner, K. (2018). Politiyofen, Poli(Sülfonik Asit difenil Anilin) Ve Nanokompozitlerinin Termoelektrik Özelliklerine Manyetik Alanın Etkisinin Araştırılması. [Unpublished doctoral dissertation] Yıldız Technical University.

International Energy Agency (2023, November) *Energy Efficiency 2023* https://www.iea.org/reports/energy-efficiency-2023

Jönsson, S. K. M., Birgerson, J., Crispin, X., Greczynski, G., Osikowicz, W., Van Der Gon, A. D., & Fahlman, M. (2003). The effects of solvents on the morphology and sheet resistance in poly (3, 4-ethylenedioxythiophene)–polystyrenesulfonic acid (PEDOT–PSS) films. Synthetic metals, 139(1), 1-10.doi: 10.1016/S0379-6779(02)01259-6

Kaya, A. S. (2021). İletken Polimer ve Metal Parçacık İçeren Kompozit Filmler. [Unpublished master dissertation] Bursa Uludağ University.

Kazemi, F., Naghib, S. M., Zare, Y., & Rhee, K. Y. (2021). Biosensing applications of polyaniline (PANI)-based nanocomposites: A review. Polymer Reviews, 61(3), 553-597.

Lee, H. (2013). The Thomson Effect and the Ideal Equation on Thermoelectric Coolers. *Energy* 56:61-69. doi: 10.1016/j.energy.2013.04.049.

Li, T., Saadatnia, Z., Chen, T., Chen, J. X. M., Shi, H. T. H., & Naguib, H. E. (2023). Facile material extrusion of 3D wearable conductive-polymer micro-super-capacitors. Additive Manufacturing, 74, 103714. doi: 10.1016/j.addma.2023.103714

Li, W., Poudel, B., Kishore, R. A., Nozariasbmarz, A., Liu, N., Zhang, Y., & Priya, S. (2023). Toward high conversion efficiency of thermoelectric modules through synergistical optimization of layered materials. Advanced Materials, 35(20), 2210407.doi: 10.1002/adma.202210407

Liang, Y., Ernst, M., Brings, F., Kireev, D., Maybeck, V., Offenhäusser, A., & Mayer D. (2018). “High Performance Flexible Organic Electrochemical Transistors for Monitoring Cardiac Action Potential”. *Advanced Healthcare Materials* 7(19):1800304. doi: 10.1002/adhm.201800304.

Liu, J., Wang, X., Li, D., Coates, N. E., Segalman, R. A., & Cahill. D. G. (2015). “Thermal Conductivity and Elastic Constants of PEDOT:PSS with High Electrical Conductivity”. *Macromolecules* 48(3):585-91. doi: 10.1021/ma502099t.

Liu, X., Du, Y., Meng, Q., Shen, S. Z., & Xu, J. (2019.) “Flexible Thermoelectric Power Generators Fabricated Using Graphene/PEDOT:PSS Nanocomposite Films”. *Journal of Materials Science: Materials in Electronics* 30(23):20369-75. doi: 10.1007/s10854-019-02280-2.

Liu, Y.X., Liu, H.H., Wang, J.P., & Zhang. X.X. (2017). Thermoelectric Behavior of PEDOT:PSS/CNT/Graphene Composites. *Journal of Polymer Engineering* 38(4):381-89. doi: 10.1515/polyeng-2017-0179.

Lu, B., Yuk, H., Lin, S., Jian, N., Qu, K., Xu, J., & Zhao X. (2019). Pure PEDOT:PSS Hydrogels. *Nature Communications* 10(1):1043. doi: 10.1038/s41467-019-09003-5.

Mammadov, B. (2023). Termoelektrik Modüllerin Performansına Etki Eden Faktörlerin İncelenmesi. [Unpublished master dissertation] National Defence University

Manjunath, K., & S. C. Kaushik. (2014). Second Law Thermodynamic Study of Heat Exchangers: A Review. *Renewable and Sustainable Energy Reviews* 40:348-74. doi: 10.1016/j.rser.2014.07.186.

Mannayil, J., Methattel Raman, S., Sankaran, J., Raman, R., & Madambi Kunjukutan Ezhuthachan, J. (2018). Solution processable PEDOT: PSS/multiwalled carbon nanotube composite films for flexible electrode applications. physica status solidi (a), 215(18), 1701003. doi: 10.1002/pssa.201701003.

Mutlu, D., & Karagöz, İ. (2023). Akıllı Malzeme Olarak Polimerler Ve Uygulamalari. *Konya Journal of Engineering Sciences* 11(1):274-99. doi: 10.36306/konjes.1106955.

Nezakati, T., Seifalian, A., Tan, A., & Seifalian, A. M. (2018). Conductive polymers: opportunities and challenges in biomedical applications. Chemical reviews, 118(14), 6766-6843. doi: 10.1021/acs.chemrev.6b00275.

Özbağ, S. (2010). İletken Polimerlerin Karakterizasyonu. [Unpublished master dissertation] Harran University.

Park, D., Kim, M., & Kim, J. (2020). Fabrication of PEDOT:PSS/Ag2Se Nanowires for Polymer-Based Thermoelectric Applications. *Polymers* 12(12):2932. doi: 10.3390/polym12122932.

Patil, B. H., Jagadale, A. D., & Lokhande, C. D. (2012). Synthesis of Polythiophene Thin Films by Simple Successive Ionic Layer Adsorption and Reaction (SILAR) Method for Supercapacitor Application. *Synthetic Metals* 162(15-16):1400-1405. doi: 10.1016/j.synthmet.2012.05.023.

Pillai, A. S., Chandran A., & Peethambharan, S. K. (2021). MWCNT Ink with PEDOT:PSS as a Multifunctional Additive for Energy Efficient Flexible Heating Applications. *Applied Materials Today* 23:100987. doi: 10.1016/j.apmt.2021.100987.

Pinto, C. S., Souza, V. H. R., Schmidt, A., & Zarbin, A. J. G. (2023). PSS-Free PEDOT and PEDOT/Graphene Transparent Films: Synthesis, Characterization and Electrochromism. *Synthetic Metals* 293:117259. doi: 10.1016/j.synthmet.2022.117259.

Pradhan, S., & Yadavalli, V. K. (2024). A Dual Function Conductive Nano Ink for Printed Electronics Connections. *Organic Electronics* 124:106959. doi: 10.1016/j.orgel.2023.106959.

Sasaki, Y., Lyu, X., Tang W., Wu, H., & Minami T. (2021). Polythiophene-Based Chemical Sensors: Toward On-Site Supramolecular Analytical Devices. *Bulletin of the Chemical Society of Japan* 94(11):2613-22. doi: 10.1246/bcsj.20210265.

Shi, X.L., Zou, J., & Chen, Z.G. (2020). "Advanced Thermoelectric Design: From Materials and Structures to Devices". *Chemical Reviews* 120(15):7399-7515. doi: 10.1021/acs.chemrev.0c00026.

Su, Z., Jin, Y., Wang, H., Li, Z., Huang, L., & Wang, H. (2022). PEDOT: PSS and its composites for flexible supercapacitors. ACS Applied Energy Materials, 5(10), 11915-11932.doi: 10.1021/acsaem.2c01524.

Ritchie H., and Rosado P., (2020, July). *Explore global data on where our energy comes from, and how this is changing.* https://ourworldindata.org/energy-mix

Usta, H., & Kirmaci, V. (2002). Termoelektrik Etkiler Ve Soğutma Etkinliğinin Uygulanması. Teknoloji, 5.

VAHAPOĞLU, V. (2013). Kauçuk türü malzemeler: sınıflandırma. Mehmet Akif Ersoy Üniversitesi Fen Bilimleri Enstitüsü Dergisi, 4(1), 25-34.

Wan, J., Xia, Y., Fang, J., Zhang, Z., Xu, B., Wang, J., Ai, L., Song, W., Hui, K.N., Fan, X., & Li, Y. (2021). Solution-Processed Transparent Conducting Electrodes for Flexible Organic Solar Cells with 16.61% Efficiency. *Nano-Micro Letters* 13(1):44. doi: 10.1007/s40820-020-00566-3.

Wang, Y. (2009). Research Progress on a Novel Conductive Polymer–Poly(3,4-Ethylenedioxythiophene) (PEDOT). *Journal of Physics: Conference Series* 152:012023. doi: 10.1088/1742-6596/152/1/012023.

Xin, X., Yu, J., Gao, N., Xue, Z., Zhang, W., Xu, J., & Chen, S. (2021). Freeze-drying and mechanical redispersion of aqueous PEDOT: PSS. Journal of Applied Polymer Science, 138(5), 49774. doi: 10.1002/app.49774.

Xu, Z., Song, J., Liu, B., Lv, S., Gao, F., Luo, X., & Wang, P. (2021). A conducting polymer PEDOT: PSS hydrogel based wearable sensor for accurate uric acid detection in human sweat. Sensors and Actuators B: Chemical, 348, 130674. doi: 10.1016/j.snb.2021.130674.

Yao, C. J., Zhang, H. L., & Zhang, Q. (2019). Recent progress in thermoelectric materials based on conjugated polymers. Polymers, 11(1), 107. doi: 10.3390/polym11010107.

Yuk, H., Lu, B., Lin, S., Qu, K., Xu, J., Luo, J., & Zhao, X. (2020). 3D printing of conducting polymers. Nature communications, 11(1), 1604. doi: 10.1038/s41467-020-15316-7.

Zarei, M., Samimi, A., Khorram, M., Abdi, M. M., & Golestaneh, S. I. (2021). Fabrication and characterization of conductive polypyrrole/chitosan/collagen electrospun nanofiber scaffold for tissue engineering application. International Journal of Biological Macromolecules, 168, 175-186. doi: 10.1016/j.ijbiomac.2020.12.031.

Zhang, X., MacDiarmid, A. G., & Manohar, S. K. (2005). Chemical synthesis of PEDOT nanofibers. Chemical communications, (42), 5328-5330. doi: 10.1039/b511290g.